

**IDENTIFICATION AND CONTROL OF
GLASS FURNACE**

BY

MOHAMMED ABDUL HAI

A Thesis Presented to the
DEANSHIP OF GRADUATE STUDIES

KING FAHD UNIVERSITY OF PETROLEUM & MINERALS

DHAHRAN, SAUDI ARABIA

In Partial Fulfillment of the
Requirements for the Degree of

MASTER OF SCIENCE

In

SYSTEMS ENGINEERING

MAY 2013

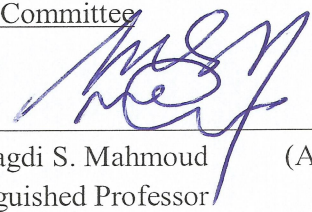
KING FAHD UNIVERSITY OF PETROLEUM & MINERALS

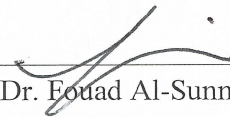
DHAHRAN 31261, SAUDI ARABIA

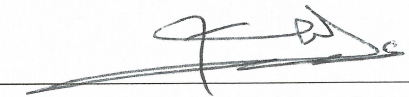
DEANSHIP OF GRADUATE STUDIES

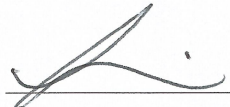
This thesis, written by **MOHAMMED ABDUL HAI** under the direction of his thesis advisor and approved by his thesis committee, has been presented to and accepted by the Dean of Graduate Studies, in partial fulfillment of the requirements for the degree of **MASTER OF SCIENCE IN SYSTEMS ENGINEERING**.

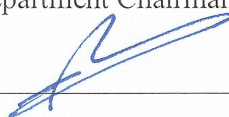
Thesis Committee


Dr. Magdi S. Mahmoud (Advisor)
Distinguished Professor


Dr. Fouad Al-Sunni (Member)
Professor & Chairman


Dr. Abdul Wahid Al-Saif (Member)
Associate Professor


Dr. Fouad Al-Sunni
(Department Chairman)


Dr. Salam A. Zummo
(Dean of Graduate Studies)

10/6/13
Date



© MOHAMMED ABDUL HAI

2013

*This Thesis is dedicated
to
My Beloved Parents, Brothers, & Sisters*

بِسْمِ اللَّهِ الرَّحْمَنِ الرَّحِيمِ

اقْرَأْ بِاسْمِ رَبِّكَ الَّذِي خَلَقَ ① خَلَقَ الْإِنْسَانَ مِنْ عَلَقٍ ② اقْرَأْ وَرَبُّكَ الْأَكْرَمُ ③
الَّذِي عَلَّمَ بِالْقَلَمِ ④ عَلَّمَ الْإِنْسَانَ مَا لَمْ يَعْلَمْ ⑤

1. Read! In the Name of Your Lord, who has created (all that exists),
2. has created man from a clot (a piece of thick coagulated blood).
3. Read! and Your Lord is the Most Generous,
4. who has taught (the writing) by the pen [the first person to write was Prophet Idrees (Enoch)],
5. has taught man that which He knew not.

(Quran 96: 1-5)

اللَّهُمَّ انْفَعْنِي بِمَا عَلَّمْتَنِي ، وَعَلِّمْنِي مَا يَنْفَعُنِي ، وَزِدْنِي عِلْمًا-

“O Allah, benefit me with what You have taught me, and teach me that which benefit me, and increase me in knowledge.”

ACKNOWLEDGMENTS

In the name of Allaah, the Most Beneficent, the Most Merciful.

All the praise is for Allaah (subhanahu wa ta'ala), the One and the only God, the Cherisher and Sustainer of the worlds, none is worthy of worship but Him. Peace and blessings be upon Prophet Muhammad (sallallahu alaihi wa sallam), and upon his children, wives and companions. My thanks to King Fahd University of Petroleum and Minerals (KFUPM) for providing a great environment for education and research. I would also like to thank the Deanship of Scientific Research (DSR) at KFUPM for financial support through research group project RG-1105-1.

I am grateful to my thesis advisor Dr. Magdi S. Mahmoud for his guidance, encouragement and patience during the tenure of my MS and especially during the thesis work. I would like to recognize the members of my thesis committee viz. Dr. Fouad Al-Sunni and Dr. Abdul-Wahid Al-Saif for giving their valuable time and help. I owe unforgettable favors of Dr. Magdi, Dr. Sami Elfrik and Dr. Fouad for standing by me and supporting me through the tough times.

I thank Allaah for all He has provided me, for accepting my supplication for studying in KFUPM, and having good companions, and for helping me in finishing my MS degree successfully.

I extend my gratitude and thanks to my parents Mr. and Mrs. Mohammed Abdul Aleem, from the bottom of my heart for giving me good upbringing, good education, for their immense hard work, patience, love, care and supplications for me. I would like to give special thanks to my mother for the encouragement she had given me to pursue higher education. My brothers (Mohammed Abdul Khaliq, Mohammed Shoaib, Mohammed Abdul Aziz), and sisters too share the same acknowledgements for their support. It would not be wrong to say that they have worked more than me, in making me what I am today. I would also like to acknowledge my eldest Aunt and her son Ahmed Al-Naquib for their supplications. I ask Allaah to reward all of them with the best in this world and the hereafter, aameen.

I credit my friends Muhammad Sabih, Masood Hussain, Hamedullah Baig, Ghufraan Ahmed, Arief Barakah, and Ahmed Tayyab, for their timely assistance and help.

I am obliged to all the brothers who supported me during my stay in Saudi Arabia. However I would especially like to mention the following brothers for their concern, motivation, valuable discussions, advices, moral support, favors, and for making my stay at KFUPM memorable and pleasant. Abdul Azeem Siddiqui, Abdul Baqi, Abdul Malik, Abdur Rahman Aravind, Akber Ali, Amer Bin Ziyad, Azharuddin Farooqui, Javed Ali, Khaleel Ahmed, Mohsin Ali, Muhammad Sabih, Rizwanullah Hussaini, Sameer Hussain, Touseef Hussain, Wajahat Kamal, Younus Siddiqui and Zabiullah.

TABLE OF CONTENTS

LIST OF FIGURES	vii
LIST OF TABLES	x
ABSTRACT (English)	xi
ABSTRACT (Arabic)	xii
Chapter 1 INTRODUCTION	1
1.1 Overview of Glass Furnace	1
1.2 Thesis Objectives	5
1.3 Thesis Organization	6
Chapter 2 LITERATURE SURVEY	7
2.1 Modeling and Identification	7

2.1.1	Empirical Modeling OR Black-Box Modeling	8
2.1.2	First Principles based Modeling	10
2.2	Control Techniques	14
Chapter 3	SYSTEM IDENTIFICATION	18
3.1	Introduction	18
3.2	State-Space Identification	21
3.2.1	Subspace Identification Method	22
3.2.2	Prediction Error Method (PEM)	23
3.3	System Identification of the Glass Furnace	24
3.3.1	Data Analysis	25
3.3.2	Linear and Nonlinear Identification	28
3.3.3	Identification using PEM and N4SID Methods	30
3.3.4	Simulation Results of Identification through PEM	32
3.4	Summary	34
Chapter 4	OPTIMAL CONTROL & ROBUST CONTROL	37
4.1	Introduction to Optimal Control	37
4.2	Linear Quadratic Regulator (LQR)	38

4.2.1	Simulation Results	41
4.3	Linear Quadratic Gaussian Regulator (LQGR)	47
4.3.1	Simulation Results	51
4.4	Introduction to \mathcal{H}_2 and \mathcal{H}_∞ Robust Control	55
4.5	\mathcal{H}_2 Optimal Control	59
4.5.1	Simulation Results	62
4.6	\mathcal{H}_∞ Optimal Control	65
4.6.1	Simulation Results	68
4.7	Comparison of LQR, LQGR, \mathcal{H}_2 , and \mathcal{H}_∞	71
 Chapter 5 MODEL PREDICTIVE CONTROL & ADAPTIVE CONTROL		73
5.1	Model Predictive Control	73
5.1.1	Introduction	73
5.1.2	MPC Algorithm	75
5.1.3	Simulation Results	79
5.2	Adaptive Control	83
5.2.1	Introduction	83
5.2.2	\mathcal{L}_1 Adaptive Control	85

5.2.3	Problem Formulation	87
5.2.4	Analysis of \mathcal{L}_1 Adaptive Controller	90
5.2.5	Design of the \mathcal{L}_1 Adaptive Controller: Robustness and Performance	92
5.2.6	Simulation Results	94
5.2.7	Comparison of \mathcal{L}_1 Adaptive Control and MRAC	99
Chapter 6	CONCLUSION AND FUTURE WORK	101
6.1	Conclusion	101
6.2	Future Work	103
Chapter A	APPENDIX	104
A.1	PEM model without direct feedthrough	104
A.2	PEM model with direct feedthrough	107
A.3	Preliminaries of \mathcal{L}_1 Adaptive Control	110
	REFERENCES	113
	VITAE	123

LIST OF FIGURES

1.1	Schematic of a Glass Furnace	2
3.1	Plot of Output Data: $y_1 - y_3$	25
3.2	Plot of Output Data: $y_4 - y_6$	26
3.3	Plot of Input Data: $u_1 - u_3$	26
3.4	Fitness Comparison of Linear & Non-Linear Models	29
3.5	Fitness Comparison of N4SID Models and PEM Models (with $D = 0$)	31
3.6	Fitness of PEM Model (with $D = 0$)	32
3.7	Fitness Comparison of PEM Models ($D = 0$ case, and $D \neq 0$ case)	33
3.8	OL Response: Without Feedthrough ($D = 0$) Vs. With Feedthrough ($D \neq 0$): States	35
3.9	OL Response: Without Feedthrough ($D = 0$) Vs. With Feedthrough ($D \neq 0$): Outputs	35

4.1	LQR (varying Q): State Trajectories $x_1 - x_4$	43
4.2	LQR (varying Q): State Trajectories $x_5 - x_7$	43
4.3	LQR (varying R): State Trajectories $x_1 - x_4$	44
4.4	LQR (varying R): State Trajectories $x_5 - x_7$	45
4.5	LQR: Output Trajectories of OL & CL Systems	46
4.6	LQGR - State Trajectories	54
4.7	LQGR - Output Trajectories	54
4.8	Generalized Block Diagram of the Modern Paradigm	55
4.9	\mathcal{H}_2 Control: State Trajectories of OL & CL Systems	63
4.10	\mathcal{H}_2 Control: Output Trajectories of OL & CL Systems	64
4.11	\mathcal{H}_∞ Control: State Trajectories of OL & CL Systems	69
4.12	\mathcal{H}_∞ Control: Output Trajectories of OL & CL Systems	70
4.13	Comparison of LQR, LQGR, \mathcal{H}_2 , & \mathcal{H}_∞ : Outputs $y_1 - y_4$	71
4.14	Comparison of LQR, LQGR, \mathcal{H}_2 , & \mathcal{H}_∞ : Outputs $y_5 - y_6$	72
5.1	Block Diagram of Model Predictive Controller	76
5.2	Strategy of MPC	77
5.3	Un-constrained MPC: Outputs	80

5.4	Un-constrained MPC: Control Inputs	81
5.5	Constrained MPC: Outputs	82
5.6	Constrained MPC: Control Inputs	82
5.7	Direct MRAC with State Predictor	85
5.8	Closed Loop \mathcal{L}_1 Adaptive System	86
5.9	Pole-Zero Map of Open-Loop and Desired Closed-Loop System .	95
5.10	Output y_2 with \mathcal{L}_1 Adaptive Control at various filter bandwidths	97
5.11	\mathcal{L}_1 Adaptive System: Control Input Trajectories	98
5.12	\mathcal{L}_1 Adaptive System: Output Trajectories	98
5.13	\mathcal{L}_1 Adaptive Controller Vs. MRAC: Control Input u_1	99
5.14	\mathcal{L}_1 Adaptive Controller Vs. MRAC: Output y_2	100

LIST OF TABLES

3.1	Comparison of PEM Models	34
4.1	Norm of LQR gain for different values of Q	42
4.2	Norm of LQR gain for different values of R	44
4.3	\mathcal{H}_2 Norm	63
4.4	\mathcal{H}_∞ Norm	69
5.1	N_p and N_c	79
5.2	Desired Poles of Closed-Loop System	95

THESIS ABSTRACT

Name: Mohammed Abdul Hai
Title: Identification and Control of Glass Furnace
Degree: Master of Science
Major Field: Systems Engineering
Date of Degree: May, 2013

Glass manufacturing process is a complex and non-linear process. The quality of the final glass product depends on temperature profile of the molten glass in glass melting furnace. Improper variations in the molten glass temperature affects the physical properties (for example: viscosity) of the glass. In order to maintain the quality of the product, the temperature of the molten glass in the furnace needs to be monitored and controlled by a control system. The designing and testing of a controller requires an appropriate process model that describes the process dynamics with enough accuracy. In industry, a common and general approach to obtain a process model is “identification”. In this thesis, a couple of identification techniques are used to obtain state space models of the glass furnace process. A comparative analysis of these models is carried out on the basis of model fitness, to suggest the best model for use of designing linear controllers. Multiple control techniques such as optimal control, robust control, model predictive control, and adaptive control methods are applied to the identified glass furnace model and their performances are analyzed and compared.

ملخص الأطروحة (عربي)

الاسم: محمد عبد الحي
عنوان الأطروحة: تحديد والتحكم في فرن الزجاج
الدرجة: ماجستير في العلوم الهندسية
التخصص: هندسة النظم
سنة التخرج: ٢٠١٣

تعتبر عملية تصنيع الزجاج من العمليات الصناعية المعقدة. وتعتمد جودة منتج الزجاج النهائي بصفه أساسيه على المخطط الحرارى للزجاج المنصهر فى أفران صهر الزجاج. وتتعكس التغييرات فى المخطط الحرارى سلبا على الخواص الطبيعیه للزجاج مثل اللزوجه و عليه فمن الواجب التحكم بدقه متناهيه فى المخطط الحرارى للزجاج المنصهر. ويتطلب تصميم نظام التحكم توافر نموذج رياضى يوصف ديناميكيه تصنيع الزجاج تحت ظروف التشغيل المختلفه. وتعتمد التطبيقات الصناعيه على "طرائق النمذجه العمليه" لبناء النماذج الرياضيه.

وقد أفردت هذه الأطروحه طريقتين لايجاد نماذج متغيرات الحاله فى عملية تصنيع الزجاج و قدمت تحليل مقارن لتقييم النماذج و تحديد مدى دقتها ومواءمتها لبيانات التصنيع المنشوره و مناسبتها لتصميم نظام التحكم. وقد تم اجراء خطوات التصميم طبقا لاساليب متنوعه تشمل التحكم الامثل و التحكم الصلد و التحكم التنبؤى و التحكم المطوع. وقد تم تطبيق هذه الاساليب على نماذج متغيرات الحاله المستخرجه و أجريت مقارنه النتائج وأستنباط الاسلوب الاكثر دقه.

Chapter 1

INTRODUCTION

1.1 Overview of Glass Furnace

Glass furnace is a key subsystem of glass industry as it is used for *melting of glass* (the main task in glass manufacturing). A glass furnace along with annealing ovens and forming machines represents the “hot end” (a place where the molten glass is produced and processed to produce glass products) of glass industry.

A glass furnace can be considered as a chemical reactor (a rectangular tank) where the raw materials are burnt in a confined space surrounded by refractory, at high temperatures of 1400 - 1600 °C to produce molten glass. The melting area of a glass furnace consists of a molten glass bath and a combustion chamber. The walls, floor and the roof of the melting area are made up of refractory

(which is capable of handling high temperatures). The furnace operation involves combustion, heat transfer, batch melting, glass flow patterns, etc. [1], [2]. Figure 1.1 shows the schematic of a glass furnace.

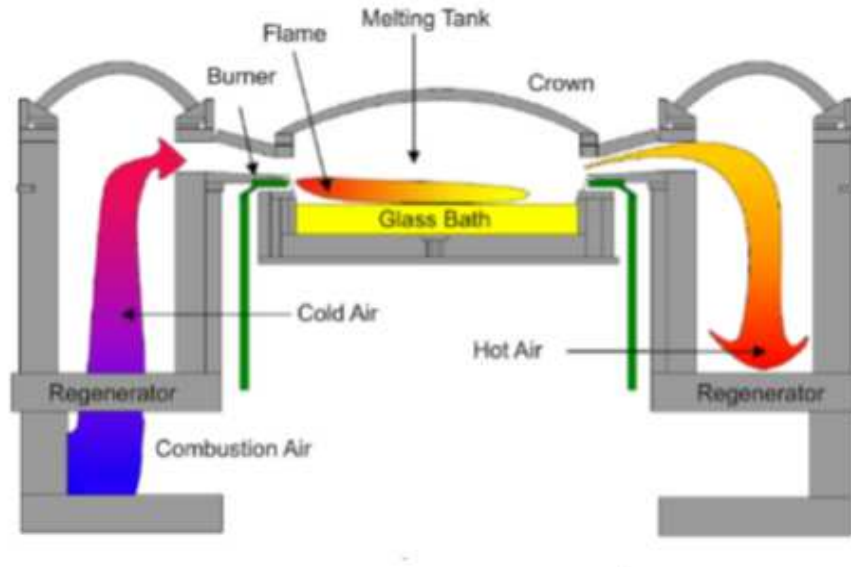


Figure 1.1: Schematic of a Glass Furnace

Glass is produced from various raw materials such as silica sand, soda ash, limestone, recycled cullet and other additives. A mixture of these raw materials is called as *batch* and it is stored and handled by a batch processing system. The batch is fed into the furnace (from one of its ends) through a continuous or intermittent feeding system and is heated to form a homogeneous melt of glass. This molten glass is then discharged through the feeders (from the opposite end of the furnace) for its further processing such as forming and polishing [3], [4], [5].

The energy (heat/temperature) required to melt the raw materials is obtained

either through combustion of fossil fuels (natural gas or oil) or through electrical resistance heating or sometimes through a combination of both fossil fuel and electrical resistance [6]. The *cost of melting* and *operation criticality* determines the type of heat source. Fossil fuel flames, directly heat the melt, mainly by heat transfer through radiations. The mass inlet streams are composed of fuel, combustion air and glass raw material. The outlet streams are flue gas and molten glass (at high temperature). Normally, a regenerator is used to recover heat from the flue gases and preheat the combustion air [1].

The glass melting process is a nonlinear, complex and slow process. The physical and chemical phenomena in this process occur at different time rates. For example, for a step change in the fuel rate, the crown temperature responds and reaches the steady state in 10 to 20 minutes while the bottom temperature takes several hours to reach the steady state. In glass furnaces, the glass melt temperatures, velocities and chemical species exhibit a slow dynamical behavior and thereby constitute to the slow dynamics of the glass melting process [7], [8].

In glass industry, the quality of the final product depends on the quality of the molten glass in the glass melting furnace. The quality of molten glass in turn depends upon the temperature of the molten glass. For example, the viscosity of the molten glass gets affected even with a temperature change of 50 to 100 °C. The change in physical properties of glass with respect to temperature creates difficulties in precise control of glass temperature. Thus, in order to maintain the product quality the temperature of the molten glass in the furnace needs to be monitored and controlled. The temperature of the molten glass is controlled

by adjusting the amount of fuel input to the furnace. A better control of the glass temperature can be achieved through monitoring and integrated control of multiple variables [2], [5].

The following variables are taken into account while modeling and control of glass furnaces [8]:

Controlled Variables or Process Variables

- Glass temperature / Bottom temperature
- Crown temperature
- Level of glass melt
- Furnace pressure
- Exhaust gas composition (e.g. NO_x) etc.

Manipulated Variables

- Air-to-fuel ratio
- Gas flow to the burners
- Batch charging speed
- Cooling air flow etc.

Measured Disturbances

- Batch composition
- Cullet ratio
- Ambient temperature etc.

Unmeasured disturbances

- Leaks
- Pollution of batch
- False air etc.

1.2 Thesis Objectives

The objectives of the thesis are:

- To perform identification of the glass furnace (Philips Glass Furnace) using linear and nonlinear identification techniques, on the basis of its experimental input-output data, and to obtain a state-space model through identification process.
- To apply the following control techniques to the identified state space model of the glass furnace.
 1. Linear Quadratic Regulator (LQR) Control
 2. Linear Quadratic Gaussian Regulator (LQGR) Control
 3. \mathcal{H}_2 Optimal Control
 4. \mathcal{H}_∞ Optimal Control
 5. Model Predictive Control (MPC)
 6. Adaptive Control

- To evaluate the performance of each of the aforementioned control techniques for the given glass furnace model and to carry out a comparative analysis of the closed-loop responses of the glass furnace system when it is controlled by these techniques.

1.3 Thesis Organization

This thesis is organized as follows:

Chapter-1 gives an overview of glass furnace and glass manufacturing process. In Chapter-2, the past work related to modeling, identification, and control of glass furnace is presented. In Chapter-3, identification of glass furnace based upon the input-output data of a real-time glass furnace system is presented. Chapter-4 gives an overview of optimal control and robust control techniques and their application to the identified glass furnace model. Chapter-5 presents two control techniques - model predictive control (MPC) and a new adaptive control technique, for control of glass furnace. The thesis is concluded by Chapter-6 in which conclusions and recommendations for future work are provided.

Chapter 2

LITERATURE SURVEY

2.1 Modeling and Identification

Broadly, there are two types of modeling techniques that have been applied so far for modeling of glass manufacturing processes [8]. They are:

1. Empirical modeling
2. First principles based modeling

2.1.1 Empirical Modeling OR Black-Box Modeling

In empirical modeling, a model of the process is developed based upon the observed behavior of the process in response to the test signals applied to the process i.e., a mathematical model of the system is developed from the input-output data of the system. This kind of modeling is also termed as *black-box modeling* or *identification* of the system. Based on the estimation methods, the identification techniques can be categorized into two: parametric estimation methods [prediction error method (PEM) & subspace identification methods (CVA, N4SID, MOESP algorithms)] and non-parametric estimation methods.

In [9] Dablemont and Gevers identify the dynamics of an industrial float glass furnace melter using a joint input output identification method.

Haber et al. [10] developed a black-box model of a continuously operating tank furnace by performing system identification on the furnace. For identification purpose, experiments were designed based on the analysis of normal operating records of the furnace. The identification was carried out without interrupting the normal production. Parameter estimation (second extended matrix method) was utilized for identification of the model and a proper model structure was obtained through repeated estimation of the parameters for different structures.

A glass furnace of end-port type was modeled through ARMAX modeling technique by Wertz and Demeuse in [11]. Several ARMAX models were identified from a record of 830 samples, representing 70 days of operation of the furnace,

with an off-line maximum likelihood algorithm. One of these models was selected based on the minimization of (Final Prediction Error) FPE criterion of Akaike and whiteness of residuals test.

Kang-Mo and Kang-Suk in [12] proposed a decision support system using Artificial Neural Networks (ANN) for a glass furnace, in which an ANN was used to identify the model. This system does not require a priori knowledge of a glass furnace process and it can be used to identify the model directly from input-output data of the process. The principle of Back-Error Propagation (BEP) was utilized in model identification and the output value was predicted from the time-lag property of a glass furnace process.

In [13] Moon and Lee developed a mathematical model of a Television (TV) glass furnace through an identification technique whose principle was based on minimizing the error between the real plant output and the model output. The structure of the model was assumed as a First-Order-Plus-Dead-Time (FOPDT) system and the parameters of the model were estimated using the root mean squares method.

Zhang et al. in [14] identified the dynamic model of a continuous large kinescope glass furnace by means of grey-box modeling technique without interrupting the normal production process. The model parameters were identified through recursive least squares method and the model was developed after repeated experiments and loss function check.

2.1.2 First Principles based Modeling

In this type of modeling, a mathematical model is derived by applying basic mass and conservation laws to the system being modeled. These models are derived from the physical knowledge of a system. First principles based modeling of glass furnace can be found in the following works: [15] - [22].

Andrea R. Holladay in her thesis work [15] developed a mathematical model for a small glass furnace. For simplification of the modeling it was assumed that the glass is well stirred and the temperature of the glass melt and refractory is homogeneous. The modeling was carried out by applying energy balance using thermodynamic and energy conservation laws and a state-space model was derived from the energy balance equations. Based on this model two types of observer designs were proposed to estimate the glass temperature from the measured combustion gas temperature. One observer was designed using only the combustion gas temperature. The other observer was designed using the refractory temperatures (floor and wall temperatures) in addition to the combustion gas temperature. The observer model was validated with a Simulink model created using the parameters developed during the formation of a state-space model from energy balance equations.

Morris in his thesis [16] extended the work of Holladay [15] by eliminating the assumptions (homogeneous temperature of glass and refractory) made by Holladay, to obtain a more accurate model. A state-space model of an end-fired small glass furnace was developed based on finite element analysis (advanced mod-

eling technique) in which subsystems are created within a system (the furnace was divided longitudinally into two zones). Overall, the furnace is divided into 24 volumes and the temperature of each volume is considered as a state variable while developing the state-space model. A set of assumptions was made while developing the model; one of the assumptions being “uniform temperature within each volume of glass, refractory and gas” to obtain simple heat transfer equations. The developed model was simulated and validated using the real furnace data of a similar small tank furnace at Fenton Art Glass Company.

Liu and Larry in their work [17] developed a state-space model of a small fiberglass furnace through energy balance approach by dividing the furnace into six zones and by considering few assumptions.

CFD Modeling

In this type of modeling, a mathematical model is developed from the first-principles (i.e. basic physical laws) by utilizing Computational Fluid Dynamics (CFD) techniques. This type of model is known as CFD model.

The advantages of the basic first principles based modeling (CFD modeling) are: a system can be modeled over its wide operating ranges without the need of any experimental tests on the system being modeled; these models are accurate and they provide a direct physical insight of the system. But, they have certain drawbacks: they are complicated and they consume a lot of CPU time

to simulate the dynamics of the system with sufficient accuracy. Due to this, such models cannot be used in applications which require short computation time (for example model-based control). An accurate CFD model is obtained at the expense of complexity of the model (i.e., complexity of the model directly depends on the accuracy of modeling).

These drawbacks are eliminated by simplifying the first principles based modeling.

A simplified first principles modeling of glass furnace for control and real time simulation was developed by Olivier Auchet et al. in [18]. This method is based on zonal approach and it overcomes the drawbacks of black-box modeling and classical CFD modeling. In zonal approach, the whole system is spatially decomposed into macroscopic zones where coarse uniformity assumptions are made and then these zones are modeled using the simple mass and energy balance equations.

An alternative of obtaining simplified first principles based models is to reduce the complicated CFD models by using proper orthogonal decomposition (POD) [18]. This type of modeling technique has been proposed by Backx et al. in [19]. In this modeling technique, initially, the CFD model of the glass furnace process was obtained and then this initial model was reduced to a relatively low order state space model by using POD-based techniques. With this technique the glass melting process can be modeled over wide operating ranges with limited testing.

A similar kind of modeling was also proposed by Leendert Huisman [7], Schobben [20] and Wattamwar [21] to obtain a fast and reduced simulation model for estimation and control of glass melt temperatures in glass melting tanks and glass melt feeders. In these works, fast reduced simulation model of a glass furnace was derived from detailed first principles model (CFD model) by using POD technique in combination with system identification.

The simplified first principles modeling reduces the computation time and develops rapid models which predict the dynamic behavior of the system faster than real time prediction. These reduced models are computationally faster than the basic CFD models and are capable of providing sufficiently accurate estimates of glass melt temperature profiles for model based control applications where a rapid model is desired for the implementation of control. An application of simplified first principles model of combustion chamber of a glass furnace in model predictive control (MPC) of glass furnace has been reported by Auchet et al. in [22].

Fuzzy logic approach of modeling glass furnaces has been discussed in the following works:

Moon and Lee in [2] proposed a modeling technique for a glass furnace, in which the linear part of the furnace dynamics was modeled by a First-Order-Plus-Dead-Time (FOPDT) system and the nonlinear part of the furnace was modeled by fuzzy logic system. Hadjili et al. in [23] presented nonlinear identification through fuzzy logic system (Takagi-Sugeno fuzzy system approach) to

model a glass furnace process between the gas input and the throat temperature output. An architecture for the operation of a recuperative-type glass furnace is presented in [24]. This architecture involves process optimization along with process modeling where the modeling is carried out by fuzzy learning system.

2.2 Control Techniques

In previous works, various control techniques have been proposed for various glass furnace models and some of these control techniques have been successfully implemented on industrial glass furnaces. Let us take an overlook of these works.

A conventional multi-loop control method based on an identified model of First Order Plus Dead Time (FOPDT) structure was proposed by Moon and Lee in [13] to control the temperature of a television (T.V.) glass furnace. This control method was practically applied to a 150 ton/day hour glass melting furnace in Samsung-Coming Company in Suwon, Korea.

In [15], Holladay presented an observer based controller to control the glass temperature of a small glass furnace. In this work the observer was designed using the state space model developed from basic conservation laws. The purpose of designing an observer was to estimate the glass temperature and use it as a feedback to the controller. Such a controller provides excellent temperature control and set point tracking.

Normally, predicted glass temperature is used as a feedback to the furnace controller. Parameters other than predicted glass temperature such as combustion gas temperature, crown temperature and refractory floor temperature can also be used as a feedback for the controller. Morris [16] presented a simple feedback control scheme for a state space model of an end-fired small glass furnace, and carried out the simulations of feedback control separately for each of the four feedback parameters (temperatures) discussed above and compared their responses. It was found that the feedback controller with floor temperature as a feedback showed a better performance than the feedback controllers based on other temperatures as feedback parameters.

An estimator-based LQR control was proposed by Liu and Larry in [17] to control the bottom glass temperature of a continuous small fiber-glass furnace. A reduced order observer/estimator was designed based on state space model of the furnace and measurement of the combustion gas temperature and the bushing plate temperature, to estimate the temperature of the molten glass at different depths in the furnace. The estimated temperature is then used as feedback to the LQR controller which controls the bottom glass temperature to desired set-points by regulating the input fuel flow rate (firing rate of burner). Huisman in [7] designed a LQG controller based on the reduced model to track a reference temperature, and to examine the relation between POD basis order and closed loop performance.

Model Predictive Control (MPC) of glass furnaces have been reported in [7], [19], [20], [22] to control the crown temperature and bottom temperature of the

glass furnace. All these applications of MPC are based on reduced CFD models. In [20] MPC was designed to control the glass temperature around a nominal operating point of furnace even if the furnace is under the influence of measured and unmeasured disturbances.

Haber et al. in [10] proposed an adaptive control technique to control the glass level in a continuously operating tank furnace. This control law was implemented using the identified model. Wertz and Demeuse [11] developed a control law (weighted minimum variance control with feed-forward compensation) based on a linear ARMAX model to control the bottom temperature of the glass furnace. This control algorithm was combined with an online identification method to form an adaptive controller. In [17] a compound adaptive control was proposed and applied on an identified model of a continuous large kinescope glass furnace. This compound adaptive control scheme included self-tuning control and modified PID control with compensator. Hill et al. [25] reported adaptive control of an industrial float glass process in which Extended Horizon Adaptive Controller (EHAC) in combination with PID controller is used to stabilize the crown temperature and minimize the gas variations. In [26] a new adaptive control scheme known as model-free adaptive (MFA) control is proposed for the control of temperature of a glass furnace. This method does not require any process model and it utilizes the artificial neural network (ANN) for the control strategy. Based on the error between the set-point and the measured process variable the neural network algorithm updates the weighting factors and provides it to the controller so that the controller takes a new action to minimize

the error.

A neural network (NN) control scheme based on hierarchically unified neural network (HUNN) architecture (integration of recurrent NN and feed-forward NN) was applied to a T.V. glass-bulb melting furnace to control its operation in [4].

Moon and Lee [2] developed a hybrid control algorithm comprising conventional PID control and fuzzy logic control to control the glass temperature (i.e. bottom temperature) of a glass melting furnace. In this work, the linear part of the furnace dynamics is modeled by a First-Order-Plus-Dead-Time (FOPDT) System and a PI controller is applied to control this linear model. The nonlinear part of the furnace is modeled and controlled by the fuzzy logic system. This hybrid control technique was successfully implemented on an actual furnace in Samsung-Corning Company in Suwon Korea.

In [24] an expert controller is applied to a fuzzy model of recuperative-type glass furnace for process optimization in which genetic algorithm is used to solve a multi objective optimization problem.

Chapter 3

SYSTEM IDENTIFICATION

3.1 Introduction

System Identification is the science that deals with developing mathematical models of physical systems from observations and measurements (experimental data) of parameters of the system. Hence, system identification can be regarded as an experimental approach to determine the dynamic model of a system. Basically, there are two types of identification techniques to identify/estimate the dynamical model of a system. They are: (i) *parametric methods* & (ii) *non-parametric methods*. Based on the method used for identification, the identified models are classified as *parametric models* and *non-parametric models*.

1. ***Parametric Identification Methods*** are techniques that estimate parameters in given model structures. Basically it is a matter of finding (by numerical search) those numerical values of the parameters that give the best agreement between the model's (simulated or predicted) output and the measured output. The parametric methods are further classified as *prediction error method* & *subspace methods*. The different types of parametric model structures are *autoregressive with exogeneous input (ARX)*, *autoregressive moving average with exogeneous input (ARMAX)*, *output error (OE)*, *Box-Jenkins (BJ)*, and *state-space* model structures.
2. ***Non-parametric Identification Methods*** are techniques that estimate model behavior without necessarily using a given parameterized model set. Typical non-parametric methods include *Correlation Analysis*, which estimates a system's impulse response, and *Spectral Analysis*, which estimates a system's frequency response.

System Identification procedure involves the following four steps for parametric identification [27]:

1. ***Acquisition of Input/Output Data***

The input-output data of a process/system is obtained by carrying out an experiment on the system under certain conditions and selection of parameters to be measured. The experiment is designed in such a way that the measured data provides maximum and useful information of the properties of the system.

2. *Selection of a Model Structure (a set of models)*

A set of candidate models is selected based on the properties of the models. This is the most important task of system identification because it requires engineering intuition, *a priori* knowledge and insight along with the mathematical properties of the models.

3. *Determining the Best Model, and Estimation of Parameters*

After obtaining the model set, a simplest model that best describes the dynamics of the system is selected from this set of models. Then, the parameters of the model are estimated based on the *error criterion* (loss function); The criterion that is used most often is the *sum of the squares of some error signals* (residuals). The values of the parameters are determined by minimizing the loss function.

4. *Validation of the Identified Model*

In this step, the identified model is validated by considering the following factors:

- the error percentage between the response of the identified model (to the validation data) and the measured output (this factor is also known as model fitness)
- the relation of the identified model to the *a priori* knowledge of the system
- whether the model is good enough for its intended use

3.2 State-Space Identification

State-space models are common representations of dynamical models and most of the industrial processes can be described accurately by discrete-time linear time-invariant (LTI) state-space models. These models are very useful for designing controllers because many control system design tools based on such type of models are available. So, in this thesis, we obtain a state-space model of the glass furnace from the experimental data by using *parametric estimation* methods, so as to design various controllers for the glass furnace process.

State-space model describes the linear difference relationship between the inputs and the outputs of the system. The basic discrete-time state-space model in innovations form is expressed by the following equations:

$$x(k+1) = Ax(k) + Bu(k) + Ke(k) \quad (3.1a)$$

$$y(k) = Cx(k) + Du(k) + e(k) \quad (3.1b)$$

where $x(k) \in \mathbb{R}^n$ is the state vector of the process at discrete time instant k and it contains the numerical values of n states, $u(k) \in \mathbb{R}^m$ is the input vector representing the values of m inputs at time instant k , $y(k) \in \mathbb{R}^l$ is the output vector representing the values of l outputs at time instant k , $e(k) \in \mathbb{R}^l$ is the noise vector.

$A \in \mathbb{R}^{n \times n}$ is the system matrix, describing the dynamics of the system; $B \in$

$\mathfrak{R}^{n \times m}$ is the input matrix, describing how the next state is influenced by the deterministic inputs; $C \in \mathfrak{R}^{l \times n}$ is the output matrix, which represents the transformation of internal state to the outside world; $D \in \mathfrak{R}^{l \times l}$ is the direct feedthrough matrix, representing the direct coupling between the input and the output (this matrix will be zero for strictly proper models); and $K \in \mathfrak{R}^{n \times l}$ is the matrix representing the noise/disturbance characteristics.

There are two basic methods for the estimation of state-space models:

1. Subspace Identification Method
2. Prediction Error Method (PEM)

3.2.1 Subspace Identification Method

The state-space matrices A , B , C , D , and K in (3.1a) & (3.1b) can be estimated directly, without first specifying any particular parameterization by efficient subspace methods. The idea behind this can be explained as follows: if the sequence of state vectors $x(k)$ were known, together with $y(k)$ and $u(k)$, (3.1b) would be a linear regression, and C and D could be estimated by the least squares method. Then $e(k)$ could be determined, and treated as a known signal in (3.1a), which then would be another linear regression model for A , B and K . Thus, once the states are known, the estimation of the state-space matrices is easy.

All states in representations like (3.1a) & (3.1b) can be formed as linear combinations of the k -step ahead predicted outputs ($k = 1, 2, \dots, n$). It is thus a matter of finding these predictors, and then selecting a basis among them. The subspace methods form an efficient and numerically reliable way of determining the predictors by projections directly on the observed data sequences.

Numerical algorithms for Subspace State-Space System Identification (N4SID):

It is a subspace-based identification method that does not use iterative search. The N4SID algorithms are always convergent (non-iterative) and numerically stable since they only make use of QR and Singular Value Decompositions. The quality of the resulting estimates may significantly depend on an auxiliary order (like a prediction horizon). It is easier to estimate state-space models directly without specifying a particular structure. This is done using N4SID.

3.2.2 Prediction Error Method (PEM)

A common and general method of estimating the parameters is the prediction error approach, where simply the parameters of the model are chosen so that the difference between the model's (predicted) output and the measured output is minimized. This method is available for all model structures. Except for the *ARX* case, the estimation involves an iterative, numerical search for the best fit.

PEM is a standard prediction error/maximum likelihood method, based on iterative minimization of a criterion. The iterations are started up at parameter values that are computed from N4SID. The parametrization of the matrices A , B , C , D , and K follows a default canonical form.

3.3 System Identification of the Glass Furnace

In this thesis, a Philips glass furnace system is considered. This glass furnace system is a multi-input multi-output (MIMO) system with three inputs and 6 outputs. The input/output experimental data of this glass furnace system is taken from SISTA's Identification Database [28]. This data consists of 1247 samples (of the respective inputs and outputs) with a sampling interval of 1 unit. The inputs and outputs of the system are listed below.

Inputs

- u_1 : heating input
- u_2 : cooling input
- u_3 : heating input

Outputs

- $y_1 - y_6$: temperature measures (readings of temperature sensors positioned in a cross section of the furnace).

The source from which this data is taken, provides neither the description of

the inputs and outputs nor their measuring units, and the data is a normalized data.

3.3.1 Data Analysis

The experimental data has been divided into two sets (one set for estimation of the model and the other set for validation of the model). The samples 1-1100 are used for estimation purpose, and the samples 601-1200 are used for validation purpose. First, the input data and the output data is plotted with respect to time as shown in figures 3.1, 3.2, & 3.3. From these plots it is observed that the input signals and output signals are not affected by an offset and hence there is no need of de-trending the data.

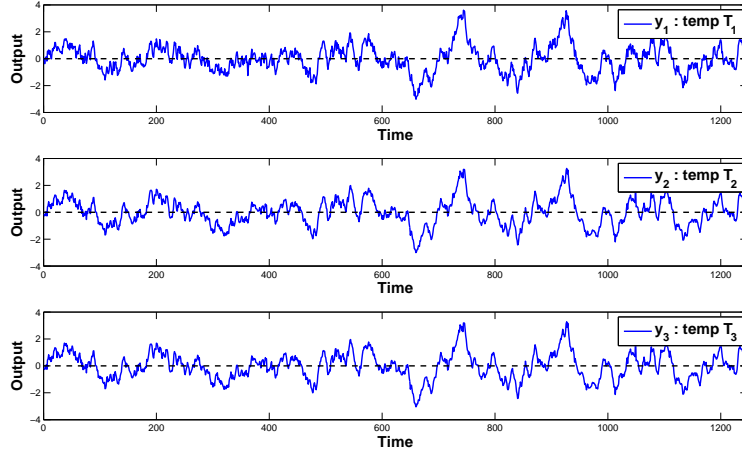


Figure 3.1: Plot of Output Data: $y_1 - y_3$

The data has been analyzed further using the function “*advice()*” from *System*

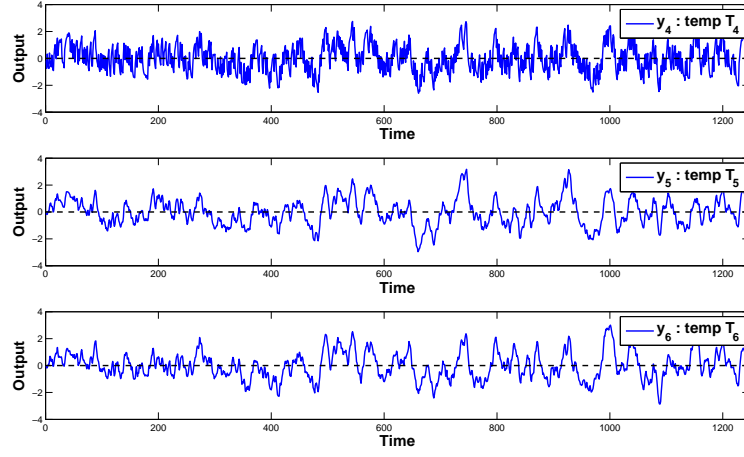


Figure 3.2: Plot of Output Data: $y_4 - y_6$

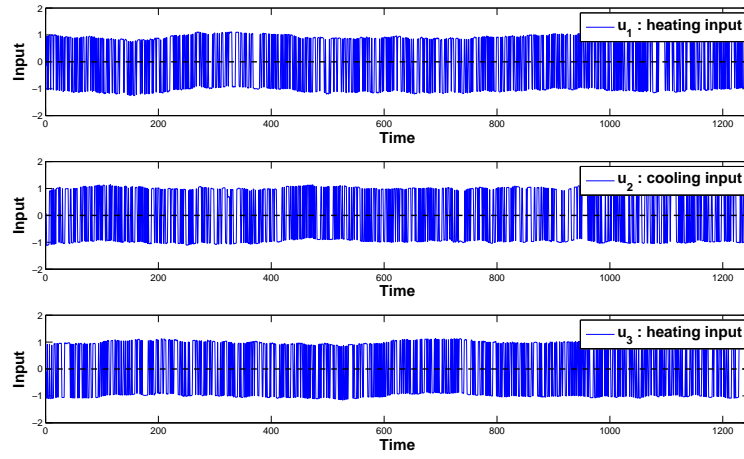


Figure 3.3: Plot of Input Data: $u_1 - u_3$

Identification Toolbox of MATLAB. On executing the command “*advice(data)*” the analysis of the data is displayed in the MATLAB Command Window as follows:

1. *The system has a direct response from inputs u_1 and u_3 at time instant k to $y(k)$. There may be two reasons for this:*

- *There is direct feedback from $y(k)$ to $u(k)$ (like a P -regulator).*

Solution: use $nk > 0$ for these inputs in state-space and input-output models.

- *The system has a direct term (relative degree zero)*

Solution: use $nk = 0$ for these inputs

2. *There is a very strong indication of feedback in the data.*

Solution: With feedback in data, it is recommended to use estimate a model with large enough disturbance model.

Based on the analysis of the data represented above, it can be inferred that there is direct feedthrough from inputs to outputs and hence the following is considered while identifying the glass furnace model from this data:

- Estimating the feedthrough from inputs u_1 and u_3 to the outputs

i.e., estimate the matrix D with $nk = [0 \ 1 \ 0]$. This implies that $D \neq 0$.

Thus, identification procedure has been carried out for *no direct feedthrough* case as well as for *direct feedthrough* case, and the models obtained in each of these

cases are analyzed and compared.

3.3.2 Linear and Nonlinear Identification

The following identification techniques are applied to the estimation data using the *System Identification Toolbox* of MATLAB.

Linear Identification techniques

- Subspace Identification Method: N4SID
- Prediction Error Method (PEM)
- MIMO ARX method

Non-Linear Identification techniques

- Non-Linear MIMO ARX method
- Non-Linear MIMO Hammerstein-Wiener method

Identification has been carried out with the identification techniques discussed above for seven different sets of estimation data (i.e., 1-600, 1-700, 1-800, 1-900, 1-1000, 1-1100, 1-1200). Validation of these identified models (obtained in each of the seven cases) has been done using the validation data set (601-1200). In validation process, the simulated (estimated) model output is compared against the validation data set and the comparison is represented in terms of the fitness % which is calculated as shown by (3.2) [54].

$$Fitness(\%) = \left(1 - \frac{\|\hat{y} - y\|}{\|y - \bar{y}\|}\right) \times 100 \quad (3.2)$$

where y is the actual or measured output, \hat{y} is the simulated output of the estimated model, $\bar{y} = mean(y)$.

Upon validation and comparison of the validation data fitness of the identified models, it is observed that the fitness of the models obtained through linear identification is relatively better than the fitness of the models obtained through nonlinear identification as shown in figure 3.4.

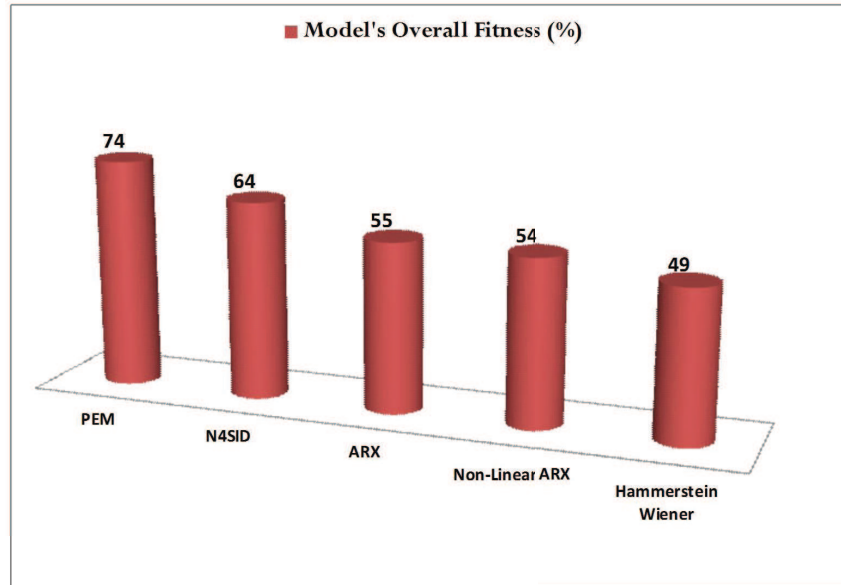


Figure 3.4: Fitness Comparison of Linear & Non-Linear Models

From figure 3.4, it is observed that among linear identified models, the validation data fitness of ARX model is less than the fitness of the N4SID and PEM models.

Besides, the ARX technique provides a polynomial model, whereas the N4SID and PEM techniques provide a state space model of the system (which is useful in designing controllers). So, we proceed with the N4SID model and PEM model for further analysis.

3.3.3 Identification using PEM and N4SID Methods

The state-space model estimated through PEM and N4SID identification techniques is in innovations form as follows:

$$x(k+1) = Ax(k) + Bu(k) + Ke(k) \quad (3.3a)$$

$$y(k) = Cx(k) + Du(k) + e(k) \quad (3.3b)$$

where $x(k)$, $u(k)$, $y(k)$, $e(k)$ are state, input, output and disturbance vectors respectively. A is the state matrix, B is the input matrix, C is the output matrix, D is the feedthrough matrix and K is the matrix representing Kalman gain. The state space identification techniques estimate the following parameters of the state space model: matrices A , B , C , K , and the initial state vector X_0 . (Note: By default, the matrix D is not estimated)

Case: Without Direct Feedthrough Term ($D = 0$)

The validation data fitness of the N4SID and PEM models (with $D = 0$) for seven different sets of estimation data is presented in figure 3.5.

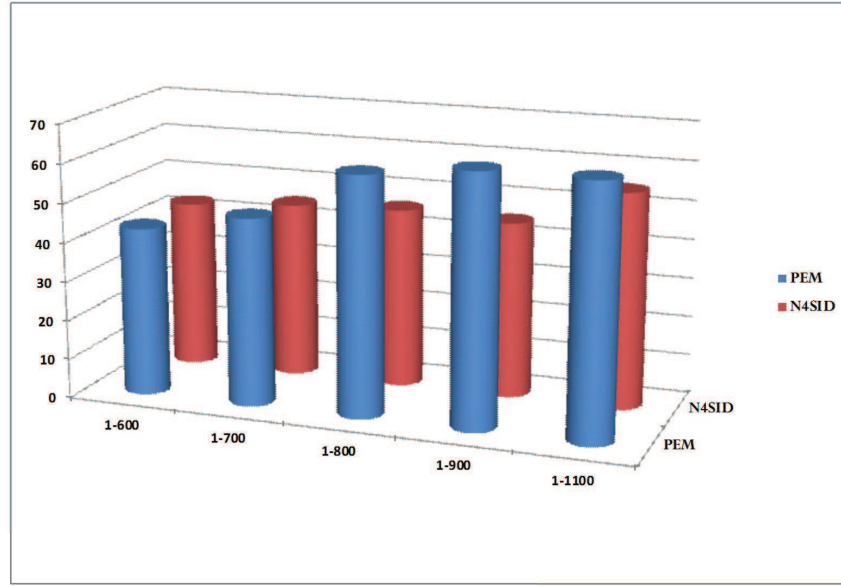


Figure 3.5: Fitness Comparison of N4SID Models and PEM Models (with $D = 0$)

It can be observed from figure 3.5 that the fitness of PEM model is better than the the fitness of N4SID model. Hence, from here onwards, the results of PEM identification method will be discussed. Among the PEM models, the model with best fitness is achieved through the estimation data set 1-1200, as illustrated in table 3.1. Figure 3.6 represents the fitness of the outputs of PEM model for this case.

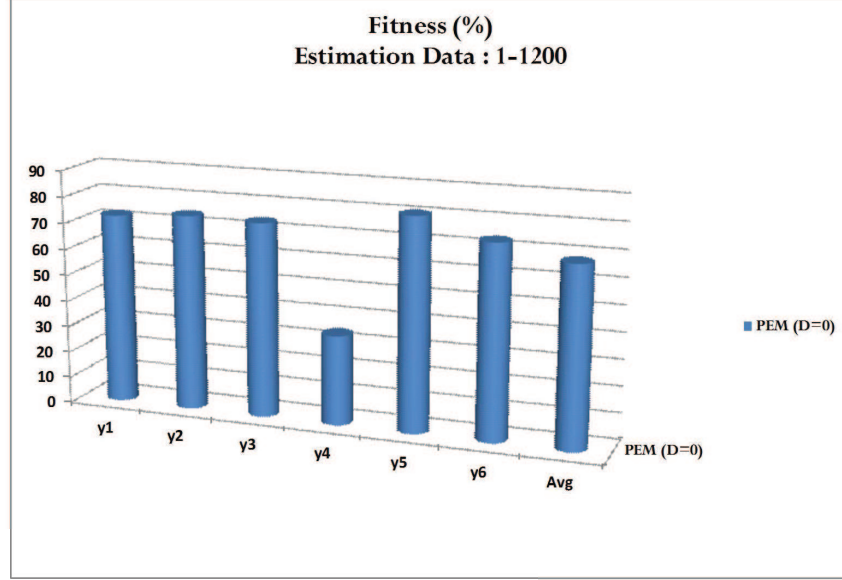


Figure 3.6: Fitness of PEM Model (with $D = 0$)

3.3.4 Simulation Results of Identification through PEM

From figure 3.6, it can be observed that the fitness level of the PEM model for the fourth output y_4 is very low. To improve this fitness, various trial and error cases based on the order of the system and estimation data were carried out but there was no improvement in the fitness. At last, considering the outcome of the foregoing data analysis, the identification is performed again, this time, by taking into account the presence of direct feedthrough from inputs.

Case: With Direct Feedthrough Term ($D \neq 0$)

Carrying out the identification process with the above considerations (with direct feedthrough from inputs u_1 and u_3 , i.e., $D \neq 0$), produced a model in which the fitness of the fourth output increased to a great extent, as well as the overall fitness of the model also increased. Figure 3.7 illustrates the comparison of fitness of PEM model without feedthrough ($D = 0$) and PEM model with feedthrough ($D \neq 0$). It is observed that the model with $D \neq 0$ has better fitness than the model with $D = 0$.

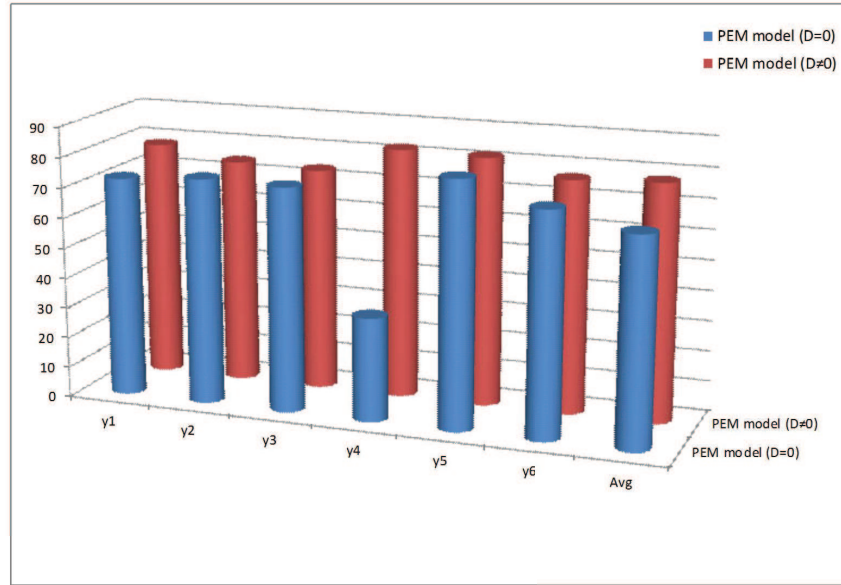


Figure 3.7: Fitness Comparison of PEM Models ($D = 0$ case, and $D \neq 0$ case)

The details (*validation data fitness, loss function, final prediction error (FPE), stability of the identified model, and order of the model*) of the PEM models obtained through the seven estimation data sets are illustrated in table 3.1.

Table 3.1: Comparison of PEM Models

Case	Estimation Data	PEM model				
		Fitness	Loss Function	FPE	Stability	Order
1.	1-600	51	1.87×10^{-14}	2.09×10^{-14}	Stable	5
2.	1-700	50	1.70×10^{-15}	1.87×10^{-15}	Stable	6
3.	1-800	68	3.19×10^{-16}	3.53×10^{-16}	Stable	7
4.	1-900	72	2.61×10^{-16}	2.85×10^{-16}	Stable	7
5.	1-1000	71	6.29×10^{-16}	6.74×10^{-16}	Unstable	6
6.	1-1100	74	9.58×10^{-16}	1.04×10^{-15}	Stable	7
7.	1-1200	78	3.52×10^{-16}	3.77×10^{-16}	Stable	7

From table 3.1, it is observed that the PEM model estimated using the data set 1-1200 is best. In this case, a 7th order, stable, state-space model with lowest loss function value (3.52×10^{-16}) and FPE value (3.77×10^{-16}) is obtained.

The open-loop responses of the PEM model without direct feedthrough $D = 0$ and with direct feedthrough $D \neq 0$ are illustrated in figures 3.8 and 3.9 which clearly indicate that the response with direct feedthrough is better than the response without feedthrough.

3.4 Summary

The data analysis of glass furnace's input-output data indicated the presence of direct feedthrough from inputs to outputs. From the simulation results of system identification of the glass furnace through various identification techniques, it is observed that linear identification provides models with good fitness. Also, the

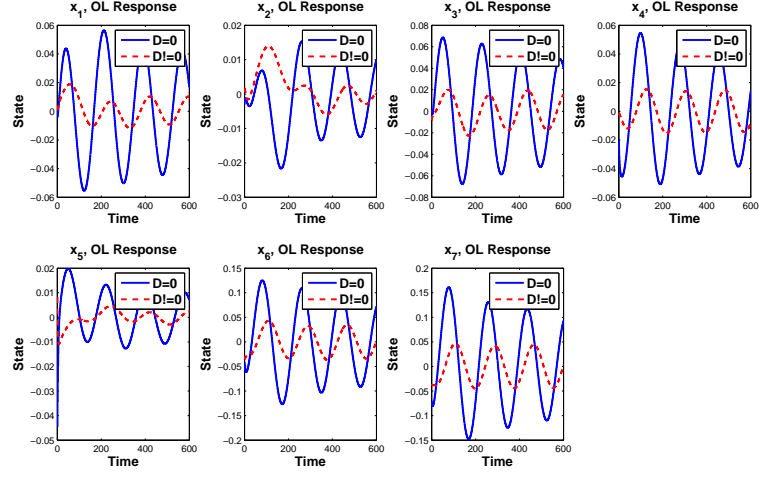


Figure 3.8: OL Response: Without Feedthrough ($D = 0$) Vs. With Feedthrough ($D \neq 0$): States

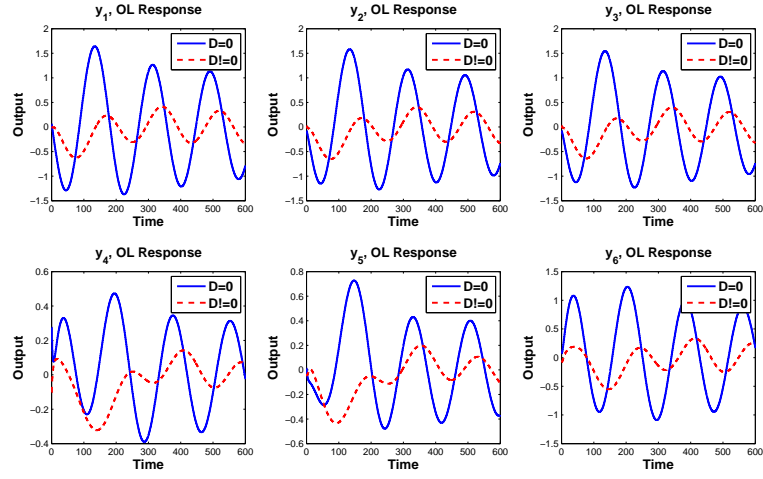


Figure 3.9: OL Response: Without Feedthrough ($D = 0$) Vs. With Feedthrough ($D \neq 0$): Outputs

PEM technique outperforms the N4SID technique in terms of model fitness. The state-space model of the glass furnace, obtained through PEM method is used for the design of various controllers such as optimal regulators (LQR, LQGR), robust controllers (\mathcal{H}_2 and \mathcal{H}_∞ controllers), model predictive controller, and adaptive controller, that are presented in chapter-4 and chapter-5.

Chapter 4

OPTIMAL CONTROL & ROBUST CONTROL

4.1 Introduction to Optimal Control

The theory of optimal control deals with the problem of finding a control law (for a given system) that helps in achieving a particular optimality criterion (in other words, the optimal control operates the system at minimum cost). This problem includes a cost functional (performance index) which is a function of state and control variables. An optimal control is a set of differential equations describing the paths of the control variables that minimize the cost functional. An optimal control problem in which the dynamics of the system are represented by a set of linear differential equations and the cost functional is represented by

a quadratic functional, is called as Linear Quadratic (LQ) optimal control problem.

4.2 Linear Quadratic Regulator (LQR)

Given a linear time-invariant (LTI) discrete-time system in state space form by the following equations:

$$\begin{aligned}x(k+1) &= Ax(k) + Bu(k) \\y(k) &= Cx(k) + Du(k) \\z(k) &= Gx(k) + Hu(k)\end{aligned}\tag{4.1}$$

where,

- $x(k) \in \mathbb{R}^n$ is the *state* vector
- $u(k) \in \mathbb{R}^m$ is the *input* vector
- $y(k) \in \mathbb{R}^p$ is the *measured output* vector
- $z(k) \in \mathbb{R}^q$ is the *controlled output* vector

Optimal LQR Control Problem can be defined as: “*finding a control law $u(k)$ that minimizes the cost function (performance index) given by (4.2)*” [29].

$$J_{\text{LQR}} = \sum_{k=0}^{\infty} \left[z^T(k)Qz(k) + \rho u^T(k)Ru(k) \right] \tag{4.2}$$

where,

- $Q \in \Re^{q \times q}$, $R \in \Re^{m \times m}$ are symmetric positive-definite matrices
- ρ is a positive constant
- the term

$$\sum_{k=0}^{\infty} \left[z^T(k) Q z(k) \right]$$

corresponds to the energy of the controlled output

- the term

$$\sum_{k=0}^{\infty} \left[u^T(k) R u(k) \right]$$

corresponds to the energy of the control signal

The most general form for the quadratic criteria is given by

$$J = \sum_{k=0}^{\infty} \left[x^T(k) \mathcal{Q} x(k) + u^T(k) \mathcal{R} u(k) + 2x^T(k) \mathcal{N} u(k) \right] \quad (4.3)$$

substituting “ $z(k) = Gx(k) + Hu(k)$ ” in (4.2) it can be seen that (4.2) is a special case of (4.3) with

$$\mathcal{Q} = G^T Q G, \quad \mathcal{R} = H^T Q H + \rho R, \quad \mathcal{N} = G^T Q H \quad (4.4)$$

LQR control utilizing state-feedback, is based on the assumption that all the states are measurable and thereby available for control. In state-feedback LQR problem, the control law is given as:

$$u(k) = -Kx(k) \quad (4.5)$$

where, $K \in \Re^{m \times n}$ is the *feedback gain* matrix given by

$$K = \mathcal{R}^{-1} \left[B^T \mathcal{P} + \mathcal{N}^T \right] \quad (4.6)$$

\mathcal{P} is the unique, symmetric, positive-definite solution to the following *algebraic Riccati equation (ARE)*

$$\mathcal{P}A + A^T \mathcal{P} - \left[\mathcal{P}B + \mathcal{N} \right] \mathcal{R}^{-1} \left[B^T \mathcal{P} + \mathcal{N}^T \right] + \mathcal{Q} = 0 \quad (4.7)$$

In a special case of (4.3) where $\mathcal{N} \equiv 0$, the optimal gain and the associated *ARE* are given as

$$K = \mathcal{R}^{-1} B^T \mathcal{P} \quad (4.8)$$

$$\mathcal{P}A + A^T \mathcal{P} - \mathcal{P}B \mathcal{R}^{-1} B^T \mathcal{P} + \mathcal{Q} = 0 \quad (4.9)$$

4.2.1 Simulation Results

The dynamics of the glass furnace system without disturbances is represented by the state-space model as

$$\begin{aligned} x(k+1) &= Ax(k) + Bu(k) \\ y(k) &= Cx(k) + Du(k) \end{aligned} \tag{4.10}$$

where $x(k) \in \mathbb{R}^7$, $u(k) \in \mathbb{R}^3$, and $y(k) \in \mathbb{R}^6$, are state, control input and measured output vectors respectively. The matrices $A \in \mathbb{R}^{7 \times 7}$, $B \in \mathbb{R}^{7 \times 3}$, $C \in \mathbb{R}^{6 \times 7}$, $D \in \mathbb{R}^{6 \times 3}$ describe the dynamics of the glass furnace system. The simulation results are provided for the case without direct feedthrough.

Case: Without Direct Feedthrough Term (i.e., $D = 0$)

LQR controller based on state feedback approach is designed for the glass furnace system, in MATLAB environment using the discrete-time function “*dlqr*(A , B , Q , R)”. The following two sets of simulations are carried out through various combinations of Q and R to investigate the performance of the controller in response to the weighting factors on states and inputs.

- R is kept constant and Q is varied: $R = I_{3 \times 3}$, $Q = \rho * I_{7 \times 7}$
- Q is kept constant and R is varied: $Q = I_{7 \times 7}$, $R = \rho * I_{3 \times 3}$

$$\mathbf{R} = \mathbf{I}_{3 \times 3}, \mathbf{Q} = \rho * \mathbf{I}_{7 \times 7}$$

In this set of simulations, five different cases of weighting matrix \mathbf{Q} are considered. The LQR gain \mathbf{K}_{lqr} and its norm obtained in each of these cases is shown in table 4.1.

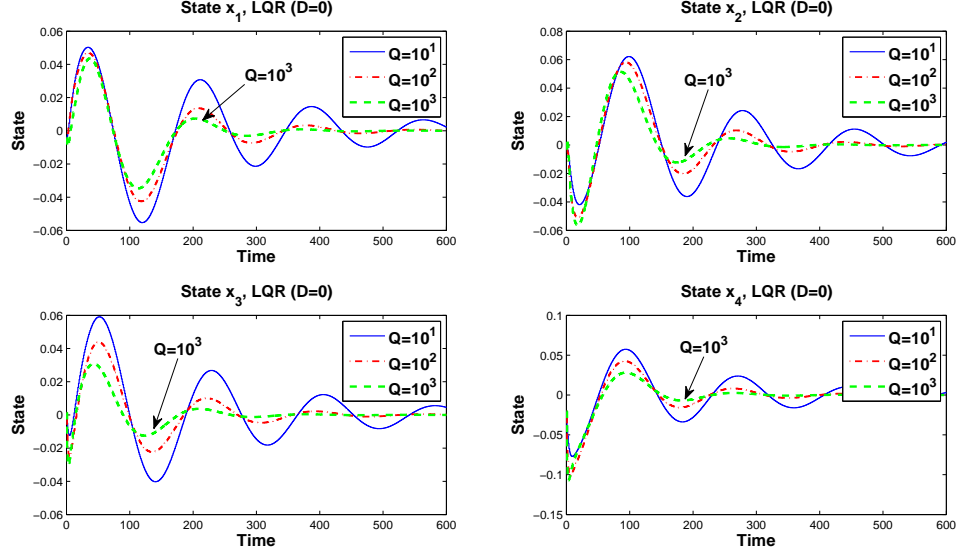
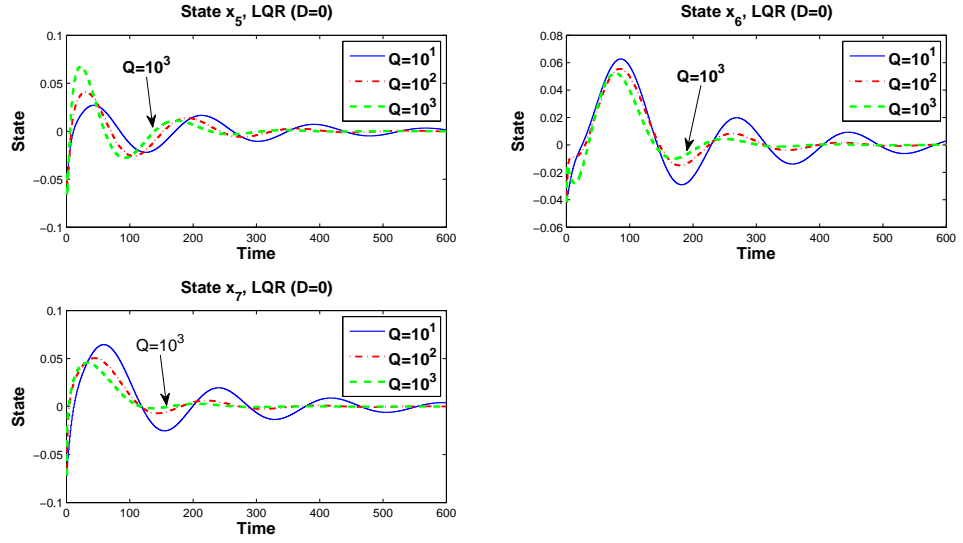
Table 4.1: Norm of LQR gain for different values of \mathbf{Q}

Case	ρ	$\mathbf{Q} = \rho * \mathbf{I}_{7 \times 7}$	$\ \mathbf{K}_{lqr}\ $
1.	1	$\mathbf{I}_{7 \times 7}$	4.2616
2.	10	$10 * \mathbf{I}_{7 \times 7}$	15.9638
3.	100	$100 * \mathbf{I}_{7 \times 7}$	53.0740
4.	1000	$1000 * \mathbf{I}_{7 \times 7}$	170.3677
5.	10000	$10000 * \mathbf{I}_{7 \times 7}$	502.5511

The closed-loop system controlled by LQR is simulated for the cases illustrated in table 4.1, and its responses are plotted. The state trajectories of the regulated closed-loop system are shown in figures 4.1 and 4.2. From the figures it is observed that more weight on the states leads to a response with less oscillations and less settling time. The case with $\mathbf{Q} = 1000 * \mathbf{I}_{7 \times 7}$ & $\mathbf{R} = \mathbf{I}_{3 \times 3}$ gives the best result but at the expense of high LQR gain \mathbf{K}_{lqr} as it can be seen in the table above.

$$\mathbf{Q} = \mathbf{I}_{7 \times 7}, \mathbf{R} = \rho * \mathbf{I}_{3 \times 3}$$

In this set of simulations, five different cases of weighting matrix \mathbf{R} are considered. The LQR gain \mathbf{K}_{lqr} and its norm obtained in each of these cases is shown in the table below.

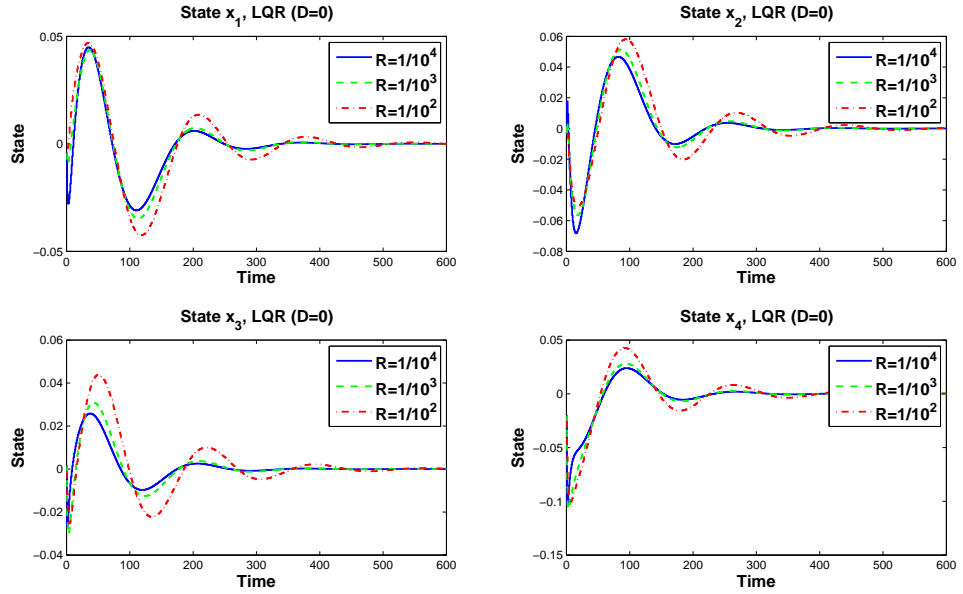
Figure 4.1: LQR (varying Q): State Trajectories $x_1 - x_4$ Figure 4.2: LQR (varying Q): State Trajectories $x_5 - x_7$

The closed-loop system controlled by LQR is simulated for the cases illustrated in table 4.1, and its responses are plotted. The state trajectories of the regulated

Table 4.2: Norm of LQR gain for different values of R

Case	ρ	$R = \rho * I_{3 \times 3}$	$\ K_{lqr}\ $
1.	0.0001	$0.0001 * I_{3 \times 3}$	502.5511
2.	0.001	$0.001 * I_{3 \times 3}$	170.3677
3.	0.01	$0.01 * I_{3 \times 3}$	53.0740
4.	0.1	$0.1 * I_{3 \times 3}$	15.9638
5.	1	$I_{3 \times 3}$	4.2616

closed-loop system are shown in the figures 4.3 and 4.4. From the figures it is observed that low weight on inputs leads to a response with less oscillations and less settling time. The case with $Q = I_{7 \times 7}$ & $R = 0.001 * I_{3 \times 3}$ gives the best result with low LQR gain K_{lqr} as it can be seen in the table above.

Figure 4.3: LQR (varying R): State Trajectories $x_1 - x_4$

From the above two simulation sets, it can be noticed that: with unity weight on control inputs, the weights on states needs to be increased in order to sta-

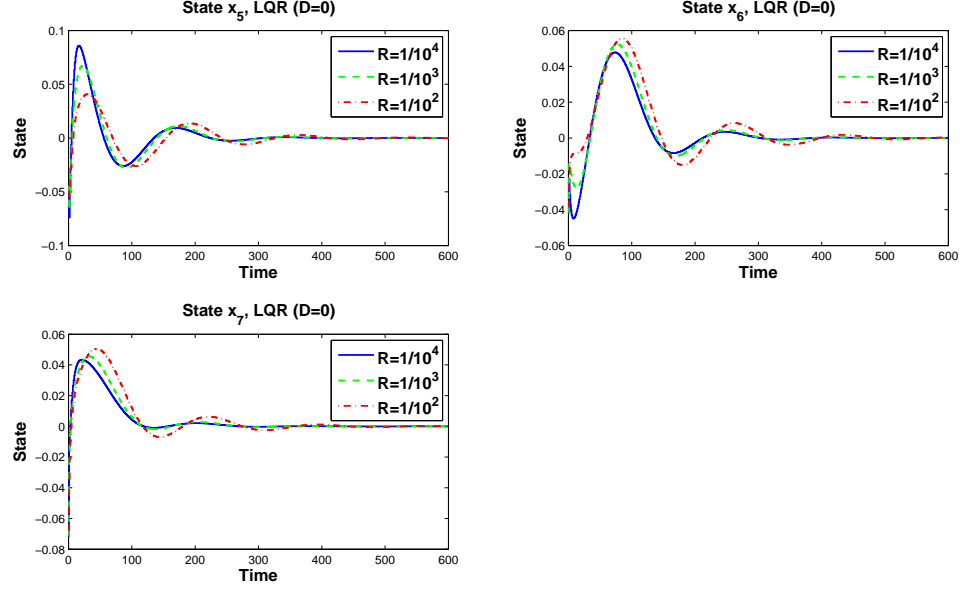


Figure 4.4: LQR (varying R): State Trajectories $x_5 - x_7$

bilize the system. An increase in weighting on states results in high LQR gain. Whereas, with unity weight on states, the weight on control inputs needs to be decreased to stabilize the system. A decrease in weighting on inputs results in high LQR gain. Thus it can be said that the LQR gain is directly proportional to the magnitude of states and inversely proportional to the magnitude of control inputs.

The output trajectories of the open-loop system and the closed-loop system are shown in figure 4.5.

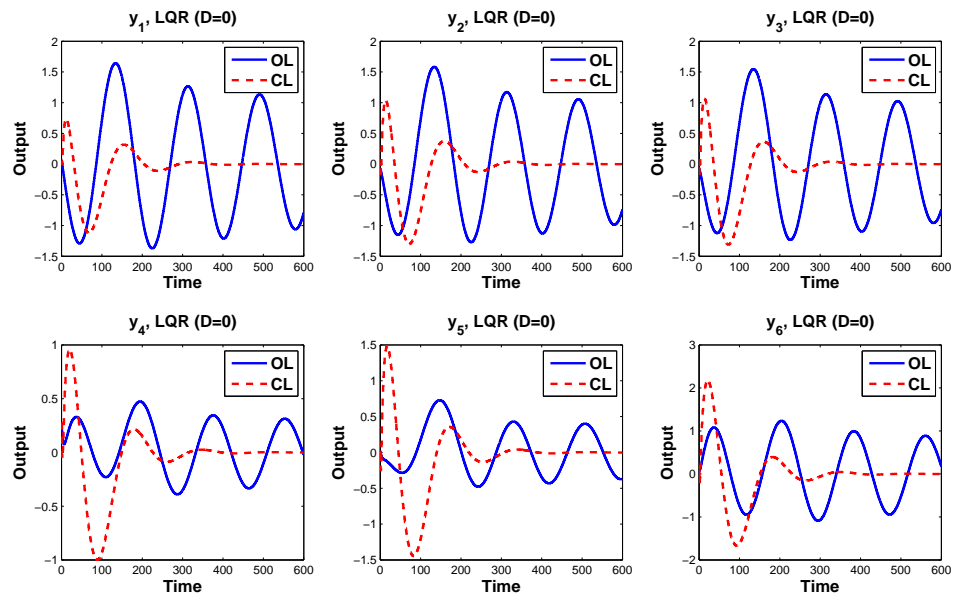


Figure 4.5: LQR: Output Trajectories of OL & CL Systems

4.3 Linear Quadratic Gaussian Regulator (LQGR)

The LQG control problem is an optimal control problem which deals with linear systems affected by white Gaussian noises and having incomplete information of its states (i.e., all the states of the system are not measurable and thus not available for feedback).

Given a linear time-invariant (LTI) discrete-time system affected by white Gaussian noises, in state-space form by the following equations:

$$\begin{aligned}x(k+1) &= Ax(k) + Bu(k) + \Gamma w(k) \\z(k) &= Gx(k) + Hu(k) \\y(k) &= Cx(k) + Du(k) + v(k)\end{aligned}\tag{4.11}$$

where,

- $x(k) \in \mathbb{R}^n$ is the *state* vector
- $u(k) \in \mathbb{R}^m$ is the *input* vector
- $y(k) \in \mathbb{R}^p$ is the *measured output* vector
- $z(k) \in \mathbb{R}^q$ is the *controlled output* vector
- $w(k)$ is the *plant noise* vector
- $v(k)$ is the *measurement noise* vector

$w(k)$ and $v(k)$ are zero-mean Gaussian white noise processes with power spectrum W and V respectively. Also, $W = W^t \geq 0$, $V = V^t \geq 0$ and

$$\left. \begin{aligned} \mathbb{E}[w(k)w^t(k)] &= W\delta(k-s) \\ \mathbb{E}[v(k)v^t(k)] &= V\delta(k-s) \\ \mathbb{E}[w(k)v^t(k)] &= 0 \end{aligned} \right\} \quad \forall k, s \in \mathfrak{R} \quad (4.12)$$

Optimal LQG Control Problem can be defined as: “*finding an observer gain matrix L that minimizes the steady-state mean square estimation error (4.13) under output feedback, and finding a control law $u(k)$ that minimizes the linear quadratic cost given by (4.2)*”.

$$\lim_{k \rightarrow \infty} \mathbb{E}\{e(k)^t e(k)\} \quad (4.13)$$

In most of the applications, some states are not measurable and hence not available for state feedback control. These unmeasurable states are optimally estimated from the outputs using the *Kalman filter*. The estimated states are then used in the optimal state feedback control law that solves the LQR problem. This accounts to the solution of a stochastic linear regulator problem with output feedback. Thus, the optimal LQG controller is a combination of linear quadratic Gaussian state estimator (Kalman Filter) and linear quadratic regulator (LQR). The optimal LQG controller is represented by the following equations

$$\dot{\hat{x}}(k) = A\hat{x}(k) + Bu(k) + L\{y(k) - C\hat{x}(k)\} \quad (4.14a)$$

$$u(k) = -K\hat{x}(k) \quad (4.14b)$$

Since the state $x(k)$ in the state feedback control law $u(k) = -Kx(k)$ is replaced with \hat{x} , the LQG controller becomes an output feedback controller.

Kalman Filter

Let the dynamics of the plant with estimated state $\hat{x}(k)$ be represented by

$$\dot{\hat{x}}(k) = A\hat{x}(k) + Bu(k) \quad (4.15)$$

then the state estimation error e and its dynamics \dot{e} are given as

$$e(k) = x(k) - \hat{x}(k) \quad (4.16a)$$

$$\dot{e}(k) = Ax(k) - A\hat{x}(k) = Ae(k) \quad (4.16b)$$

From (4.16b) it can be noticed that when the system matrix A is asymptotically stable the error $e(k)$ converges to zero for any given input $u(k)$ which implies that $\hat{x}(k)$ eventually converges to $x(k)$ as $k \rightarrow \infty$. When A is unstable e is unbounded and $\hat{x}(k)$ grows further and further apart from $x(k)$ as $k \rightarrow \infty$. To avoid this, a correction term is added to (4.15) as shown in (4.17a).

$$\dot{\hat{x}}(k) = A\hat{x}(k) + Bu(k) + L\{y(k) - \hat{y}(k)\} \quad (4.17a)$$

$$\hat{y}(k) = C\hat{x}(k) \quad (4.17b)$$

where $\hat{y}(k)$ is an estimate of $y(k)$ and $L \in \mathbb{R}^{n \times k}$ is the gain matrix through which the magnitude of the correction term may be increased or decreased. The correction term does not have any effect on the error dynamics when $\hat{x}(k)$ is equal to or very close to $x(k)$. When $\hat{x}(k)$ grows away from $x(k)$ the correction term reduces this error. Re-writing the error dynamics using (4.17a) we have

$$\begin{aligned}\dot{e}(k) &= Ax(k) - A\hat{x}(k) - L\{Cx(k) - C\hat{x}(k)\} \\ &= (A - LC)e(k)\end{aligned}\tag{4.18}$$

The error e converges to zero as long as $(A - LC)$ is stable. If A is unstable, the observer gain matrix L can be selected so that $(A - LC)$ becomes asymptotically stable. The estimator (4.17a) is known as *full-order observer* and its dynamics can be re-written as follows

$$\dot{\hat{x}}(k) = (A - LC)\hat{x}(k) + Bu(k) + Ly(k)\tag{4.19}$$

In general, a process is affected by disturbances and measurement noise; the process dynamics are then represented by (4.11). In this case if a *full-order observer* is used to estimate the states of the system, the estimation error dynamics is given as

$$\begin{aligned}\dot{e}(k) &= Ax(k) + \Gamma w(k) - A\hat{x}(k) - L\{Cx(k) + v(k) - C\hat{x}(k)\} \\ &= (A - LC)e(k) + \Gamma w(k) - Lv(k)\end{aligned}\tag{4.20}$$

Due to the addition of the noise terms the estimation error does not converge to zero even if the error system $(A - LC)$ is stable. The error covariance matrix $\mathbb{E}[e^t(k)e(k)]$ can be brought to a steady-state minimal value \mathcal{S} by selecting the observer gain matrix L as

$$L = \mathcal{S}C^tV^{-1} \quad (4.21)$$

where \mathcal{S} satisfies the following Lyapunov equation

$$(A - LC)\mathcal{S} + \mathcal{S}(A - LC)^t + \Gamma W \Gamma^t + LSL^t = 0 \quad (4.22)$$

substituting the optimal observer gain matrix (4.21) in (4.22), the following algebraic Riccati equation *ARE* is obtained

$$A\mathcal{S} + \mathcal{S}A^t + \Gamma W \Gamma^t - \mathcal{S}C^tV^{-1}C\mathcal{S} = 0 \quad (4.23)$$

If the optimal gain L described by (4.21) is utilized in the full-order observer (4.17a), then this type of estimator/observer is known as *Kalman-Bucy Filter*.

4.3.1 Simulation Results

The identified glass furnace system with plant noise and measurement noise is represented by the following state-space model as

$$\begin{aligned}
x(k+1) &= Ax(k) + Bu(k) + \Gamma w(k) \\
y(k) &= Cx(k) + v(k)
\end{aligned}
\tag{4.24}$$

Here, the LQG regulator is designed in MATLAB using the commands "kalman()" & "lqr()" and then the Simulink environment is used to implement the LQG regulator to control the glass furnace system.

LQR design:

The following weights on states and inputs are selected to design the LQR:

$$Q = 1000 * I_{7 \times 7}, \quad R = I_{3 \times 3}$$

Using the above values of Q and R in "dlqr(A,B,Q,R)" the following optimal state feedback gain is obtained:

$$K_{lqr} = \begin{bmatrix} 44.9700 & 46.5133 & -57.5760 & 47.1600 & -4.9267 & -83.8545 & 92.0909 \\ 0.5948 & 13.5638 & 17.1872 & 6.1742 & 5.7887 & -21.2406 & 11.8634 \\ -21.0232 & -26.8838 & 36.2121 & -14.2839 & -1.6134 & 28.3619 & -21.1476 \end{bmatrix}$$

Kalman Filter design:

The plant noise and measurement noise with a magnitude of 10^{-5} are generated in SIMULINK using the "random number" block whose output is a normally

(Gaussian) distributed random signal. The noise covariance data is selected as

$$Qn = \mathbb{E}[w(k)w^t(k)] = I_{6 \times 6}$$

$$Rn = \mathbb{E}[v(k)v^t(k)] = I_{6 \times 6}$$

$$Nn = \mathbb{E}[w(k)v^t(k)] = I_{6 \times 6}$$

The Kalman Filter is designed using the MATLAB command: “ $[kest, L, P] = kalman(sys, Qn, Rn, Nn)$ ”. The Kalman gain L obtained through this design is as follows

$$L = \begin{bmatrix} 0.0010 & -0.1660 & 0.1604 & -0.0010 & 0.0043 & -0.0008 \\ -0.0017 & 0.0831 & -0.0807 & 0.0029 & -0.0117 & -0.0029 \\ -0.0171 & -0.1901 & 0.1896 & 0.0052 & 0.0044 & -0.0014 \\ -0.0320 & -0.7579 & 0.7705 & 0.0113 & 0.0155 & -0.0374 \\ -0.0134 & 1.7211 & -1.6732 & 0.0019 & -0.0322 & 0.0105 \\ 0.0385 & 3.1815 & -3.2113 & -0.0080 & 0.0081 & 0.0118 \\ 0.0337 & 4.5023 & -4.5166 & -0.0112 & 0.0235 & 0.0138 \end{bmatrix}$$

Using the above values of LQR gain K and Kalman gain L , the LQG controller is formed and connected to the glass furnace system through a positive feedback loop. The optimal state and output trajectories of this closed-loop system are shown in figures 4.6 and 4.7.

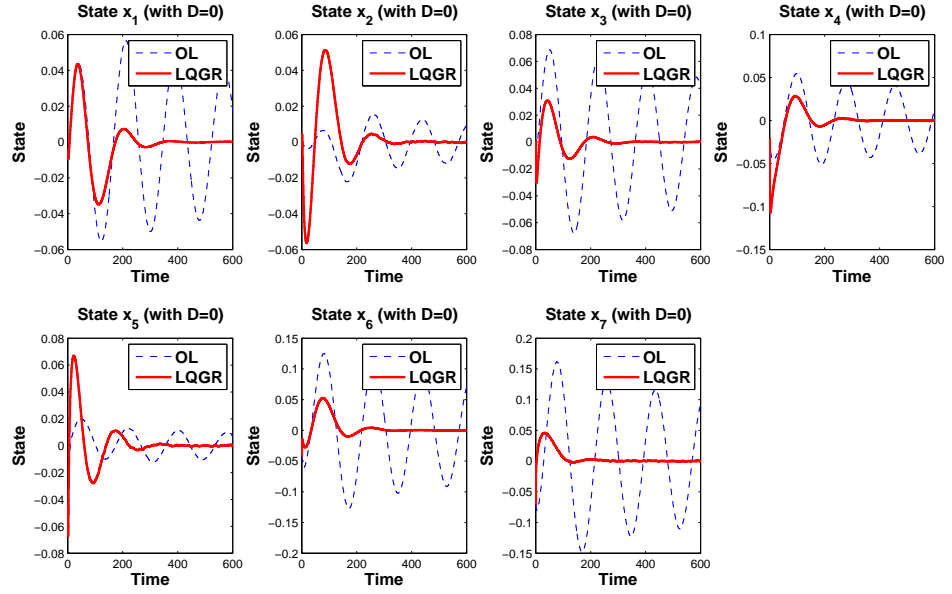


Figure 4.6: LQGR - State Trajectories

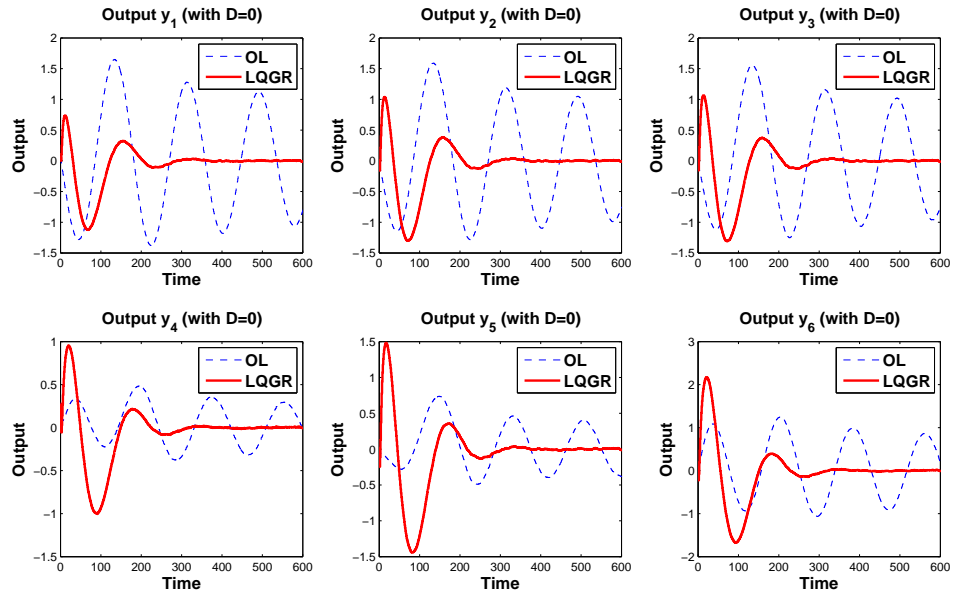


Figure 4.7: LQGR - Output Trajectories

4.4 Introduction to \mathcal{H}_2 and \mathcal{H}_∞ Robust Control

\mathcal{H}_2 and \mathcal{H}_∞ synthesis are carried out in a modern control paradigm in which both performance and robustness specifications can be incorporated in a common framework along with the controller synthesis [30]. In this paradigm, all the information of a system is cast into the generalized block diagram illustrated in figure 4.8.

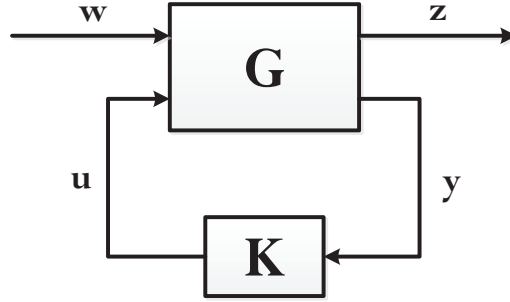


Figure 4.8: Generalized Block Diagram of the Modern Paradigm

where G is the generalized linear time-invariant plant containing all the information (for example, dynamics of the system, uncertainty models, sensor and actuator dynamics, frequency weights, etc.) required for the synthesis of the controller K ; u is the control input; y is the measured output used by the feedback controller; w comprises all the exogenous inputs to the system, such as disturbances, sensor noise, fictitious signals, etc.; z is the controlled output.

The general control problem or disturbance rejection problem in this framework is to synthesize a controller that keeps the size of the controlled outputs z small

in the presence of the disturbance inputs w . Thus, the disturbance rejection performance depends on the *size* of the closed-loop transfer function from w to z , $T_{zw}(s)$ [30]. As the effect of disturbances w on the cotnrolled outputs z depends on the *size* of the transfer function $T_{zw}(s)$, the controllers should be designed so as to minimize the *size* of the closed-loop transfer function $T_{zw}(s)$. The *size* of a transfer function is quantified by suitable norms. \mathcal{H}_2 norm and \mathcal{H}_∞ norm are the most popular norms to measure the *size* of $T_{zw}(s)$.

Let us consider the transfer function $G(s) = C(sI - A)^{-1}B$ as a system.

Definition 4.4.1 \mathcal{H}_2 Norm

The \mathcal{H}_2 norm of a system $G(s)$ is defined as follows

$$\|G(s)\|_2 = \sqrt{\frac{1}{2\pi j} \int_{-j\infty}^{j\infty} |G(j\omega)|^2 d\omega} \quad (4.25)$$

$$\|G(s)\|_2 = \sqrt{\frac{1}{2\pi} \int_{-\infty}^{\infty} \text{trace}[G(j\omega)G^*(j\omega)] d\omega} \quad (4.26)$$

where $G^*(j\omega)$ is the complex conjugate of $G(j\omega)$.

If the system $G(s)$ is driven by an independent, zero mean, unit intensity white noise, then the sum of the variances of the outputs (or mean square output) equals the square of the \mathcal{H}_2 norm of the system $G(s)$ as shown in (4.27). Hence

the \mathcal{H}_2 norm of a system gives a precise measure of the signal strength or power of the output of the system driven by unit intensity white noise.

$$\mathbb{E}\left[y^t(k)y(k)\right] = \|G(s)\|_2^2 \quad (4.27)$$

Definition 4.4.2 \mathcal{H}_∞ Norm

The \mathcal{H}_∞ norm of a system $G(s)$ is defined as follows

$$\|G(s)\|_\infty = \sup_{\omega} \sigma_{max}[G(j\omega)] \quad (4.28)$$

Here, 'sup' represents the supremum or upper bound of the function $G(j\omega)$ and therefore the \mathcal{H}_∞ norm is the maximum value of $G(j\omega)$ over all frequencies ω .

When the system is driven by a unit sinusoidal input at a particular frequency, then the corresponding sinusoidal output has a maximum value of $\sigma_{max}[G(j\omega)]$. This shows that \mathcal{H}_∞ norm is the maximum amplification of a unit sinusoidal input over all frequencies. In other words, it represents the maximum increase in energy between the input and output of a system. Since \mathcal{H}_∞ norm is an induced norm it satisfies the sub-multiplicative property of the induced norms, i.e.,

$$\|G_1 G_2\|_\infty = \|G_1\|_\infty \|G_2\|_\infty \quad (4.29)$$

Due to this property of \mathcal{H}_∞ norm, controllers that minimize $\|T_{zw}(s)\|_\infty$ are

favourable when it is desired to have loop shaping that satisfy the norm bounded robustness tests. Whereas the \mathcal{H}_2 norm is not an induced norm and due to the properties of the \mathcal{H}_2 norm, controllers that minimize $\|T_{zw}(s)\|_2$ are favourable when the disturbances are stochastic in nature.

The generalized plant G has a state-space realization as follows

$$\begin{aligned} x(k+1) &= Ax(k) + B_1w(k) + B_2u(k) \\ z(k) &= C_1x(k) + D_{11}w(k) + D_{12}u(k) \\ y(k) &= C_2x(k) + D_{21}w(k) + D_{22}u(k) \end{aligned} \tag{4.30}$$

The system (4.30) is represented in compact notation as

$$G(s) := \left[\begin{array}{c|cc} A & B_1 & B_2 \\ \hline C_1 & D_{11} & D_{12} \\ C_2 & D_{21} & D_{22} \end{array} \right] \tag{4.31}$$

$$\begin{bmatrix} z \\ y \end{bmatrix} = \begin{bmatrix} G_{11} & G_{12} \\ G_{21} & G_{22} \end{bmatrix} \begin{bmatrix} w \\ u \end{bmatrix} \tag{4.32}$$

4.5 \mathcal{H}_2 Optimal Control

\mathcal{H}_2 Optimal Control Problem is defined as: “finding a causal controller K that stabilizes the system G internally and minimizes the cost function (4.33) (minimizing this cost function is equivalent to minimizing the \mathcal{H}_2 norm of the closed-loop system (with w as input and z as output) represented by (4.34) and (4.35))” [29].

$$J_2(k) = \|F(G, K)\|_2^2 \quad (4.33)$$

Considering the partition of $G(s)$ according to (4.32), the closed-loop system

$$z = F(G, K)w \quad (4.34)$$

has the transfer function $F(G, K)$ given by

$$F(G, K) = G_{11} + G_{12}(I - KG_{22})^{-1}KG_{21} \quad (4.35)$$

known as *lower fractional transformation*.

For \mathcal{H}_2 control, the following assumptions are taken into consideration [31]:

1. $D_{11} = 0$

2. The pair (A, B_2) is stabilizable, and the pair (A, C_2) is detectable.
3. D_{21} has full row rank, and D_{12} has full column rank.
4. The matrix $\begin{bmatrix} A-sI & B_1 \\ C_2 & D_{21} \end{bmatrix}$ has full row rank for every $s = j\omega$.
5. The matrix $\begin{bmatrix} A-sI & B_2 \\ C_1 & D_{12} \end{bmatrix}$ has full column rank for every $s = j\omega$.
6. The pair (A, B_1) has no uncontrollable modes on the imaginary axis.
7. The pair (A, C_1) has no unobservable modes on the imaginary axis.

Assumption-1 (i.e., there is no direct feedthrough from w to z) is required to obtain a finite \mathcal{H}_2 norm of the closed-loop system; assumption-2 is necessary to ensure the existence of a stabilizing controller $u = Ky$; assumption-3 guarantees the non-singularity of the \mathcal{H}_2 optimal control problem (D_{21} has full row rank implies that there is “direct feedthrough” from the input u to the error signal z & D_{12} has full column rank implies that there is “direct feedthrough” from the noise input w to the measured output y); assumptions 4 & 5 along with assumption-2 guarantee that the two Hamiltonian matrices associated with the \mathcal{H}_2 problem belong to $\text{dom}(\text{Ric})$; assumptions 6 & 7 are required to guarantee the existence of the solutions to the Riccati equations which characterize the optimal controllers.

In addition, the direct feedthrough from u to y is assumed to be zero (i.e., $D_{22} = 0$) so that G_{22} is proper.

Considering the above assumptions, the transfer function of the system for \mathcal{H}_2 control problem is given as

$$G(s) := \left[\begin{array}{c|cc} A & B_1 & B_2 \\ \hline C_1 & 0 & D_{12} \\ C_2 & D_{21} & 0 \end{array} \right] \quad (4.36)$$

and, the optimal output feedback controller is given as

$$\dot{\hat{x}}(k) = A\hat{x}(k) + B_2u(k) + L\{y(k) - C_2\hat{x}(k) - D_{22}u(k)\} \quad (4.37a)$$

$$u(k) = -K\hat{x}(k) \quad (4.37b)$$

where K is the state feedback gain matrix, and L is the observer gain matrix given as follows [29]

$$K = (D_{12}D_{12}^t)^{-1}(B_2^tP + D_{12}^tC_1) \quad (4.38)$$

$$L = (SC_2^t + B_1D_{21}^t)(D_{21}D_{21}^t)^{-1} \quad (4.39)$$

where P and S are the unique, symmetric positive definite solutions of the following algebraic Riccati equations

$$A^tP + PA + C_1^tC_1 - (PB_2 + C_1^tD_{12})(D_{12}D_{12}^t)^{-1}(B_2^tP + D_{12}^tC_1) = 0 \quad (4.40)$$

$$AS + SA^t + B_1B_1^t - (SC_2^t + B_1D_{21}^t)(D_{21}D_{21}^t)^{-1}(C_2S + D_{21}B_1^t) = 0 \quad (4.41)$$

4.5.1 Simulation Results

The \mathcal{H}_2 controller is designed in MATLAB using the function “h2syn()”. This function computes a stabilizing \mathcal{H}_2 optimal controller, K ; the closed-loop system, CL ; the 2-norm of the closed-loop system, $Gam = \|T_{zw}\|_2$.

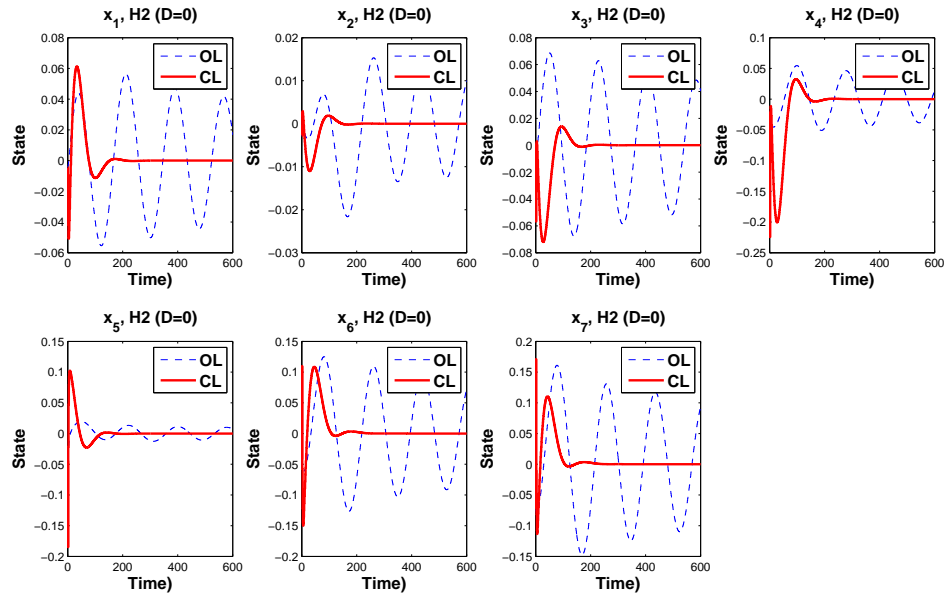
$$[K, CL, Gam, Info] = h2syn(G, Ny, Nu)$$

Here, $B_1 = K$, $B_2 = B$, $C_1 = C_2 = C$, $D_{21} = I$, $D_{22} = D$ (where, B , C , D , K are the matrices of the state-space equations (3.1a) and (3.1b)).

Simulations have been carried out by fixing the value of D_{21} at $I_{6 \times 6}$ and varying the value of D_{12} . The system response has been analyzed for five different values of D_{12} . The \mathcal{H}_2 norm of the closed-loop system obtained for these five different cases is shown in table 4.3. The state trajectories of the closed-loop system for case 1, 3 and 4 is illustrated in figure 4.9. From the response of the system and the \mathcal{H}_2 norm of the closed-loop system, it can be concluded that the \mathcal{H}_2 controller performs best at $D_{12} = 0.001 * I_{6 \times 3}$ and $D_{21} = I_{6 \times 6}$. The state trajectories and output trajectories of the open-loop and closed-loop system (with $D_{12} = 0.001 * I_{6 \times 3}$ and $D_{21} = I_{6 \times 6}$) are shown in figures 4.9 and 4.10.

Table 4.3: \mathcal{H}_2 Norm

Case	D_{12}	$\ T_{zw}\ _2$
1.	$0.001 * I_{6 \times 3}$	388.7230
2.	$0.01 * I_{6 \times 3}$	391.3776
3.	$0.1 * I_{6 \times 3}$	417.9299
4.	$I_{6 \times 3}$	864.7766
5.	$10 * I_{6 \times 3}$	2377.0000

Figure 4.9: \mathcal{H}_2 Control: State Trajectories of OL & CL Systems

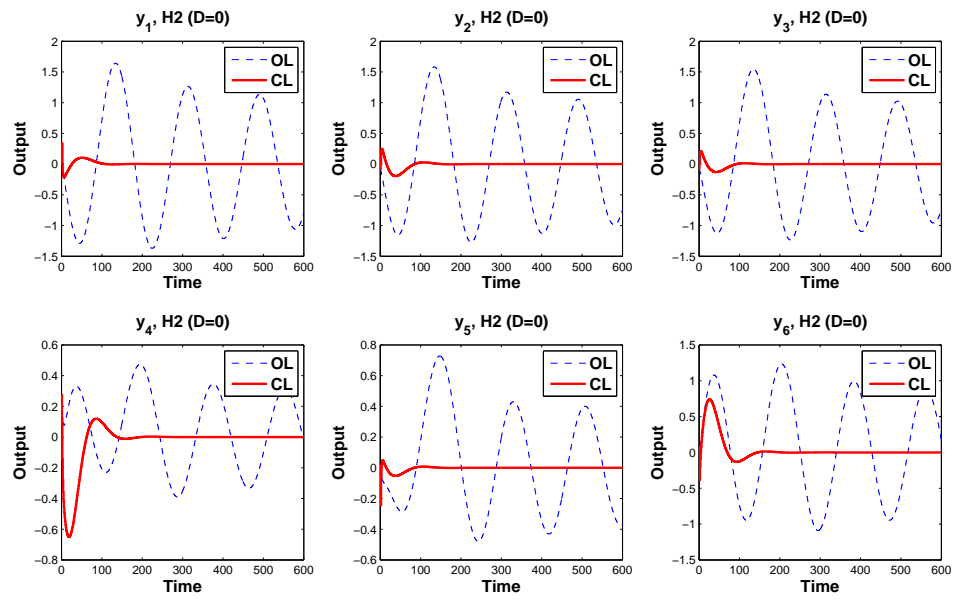


Figure 4.10: \mathcal{H}_2 Control: Output Trajectories of OL & CL Systems

4.6 \mathcal{H}_∞ Optimal Control

\mathcal{H}_∞ optimization deals with the minimization of the ∞ -norm of a frequency response function [32]. Since ∞ -norm is the worst-case gain of the system, it provides a good representation of bounds on errors and controls [33]. Mathematically, the \mathcal{H}_∞ control problem is set in the \mathcal{H}_∞ space which consists of all bounded functions that are analytic in the right-half complex plane. Though \mathcal{H}_∞ and \mathcal{H}_2 resemble each other, their results are quite different due to the dissimilarities between the properties of 2-norm and ∞ -norm.

Let the system be represented by the block diagram shown in figure 4.8. where the plant G and the controller K are assumed to be proper & real-rational and their state-space realizations are assumed to be stabilizable and detectable.

Optimal \mathcal{H}_∞ Control Problem is defined as a problem of “*finding all admissible controllers K which minimize the \mathcal{H}_∞ norm of the closed-loop system, i.e., $\|T_{zw}\|_\infty$ ”.*

If a controller stabilizes the system *internally* then it is said to be an *admissible* controller. Generally, the optimal \mathcal{H}_∞ controllers are not unique for MIMO systems. Furthermore, finding an optimal \mathcal{H}_∞ controller is often both numerically and theoretically complicated. Whereas in standard \mathcal{H}_2 theory, the optimal controller is unique and can be obtained by solving two *Riccati* equations without iterations. Knowing the achievable optimal (minimum) \mathcal{H}_∞ norm may be theoretically useful since it sets a limit on what we can achieve.

In practice, it is often not necessary and sometimes even undesirable to design an optimal controller. It is usually much cheaper to obtain controllers that are very close to the optimal ones in the norm sense, which are called as “suboptimal controllers”. A suboptimal controller possesses some properties which are better than the properties of optimal controllers, for example, lower bandwidth. Optimal \mathcal{H}_∞ controllers are more difficult to characterize than the suboptimal \mathcal{H}_∞ controllers.

Suboptimal \mathcal{H}_∞ Control Problem is defined as a problem of “*finding all the admissible controllers K such that $\|T_{zw}\|_\infty < \gamma$, given $\gamma > 0$* ”.

The \mathcal{H}_∞ solution consists of the following two Hamiltonian matrices

$$H_\infty := \begin{bmatrix} A & \gamma^{-2}B_1B_1^* - B_2B_2^* \\ -C_1^*C_1 & -A^* \end{bmatrix}, \quad J_\infty := \begin{bmatrix} A^* & \gamma^{-2}C_1^*C_1 - C_2^*C_2 \\ -B_1B_1^* & -A \end{bmatrix}$$

The transfer function of the generalized plant G is considered to have a realization of the form

$$G(s) := \left[\begin{array}{c|cc} A & B_1 & B_2 \\ \hline C_1 & 0 & D_{12} \\ C_2 & D_{21} & 0 \end{array} \right] \quad (4.42)$$

and, the following assumptions are taken into consideration

1. The pair (A, B_2) is stabilizable, and the pair (A, C_2) is detectable.
2. D_{21} has full row rank, and D_{12} has full column rank.
3. The matrix $\begin{bmatrix} A-sI & B_1 \\ C_2 & D_{21} \end{bmatrix}$ has full row rank for every $s = j\omega$.
4. The matrix $\begin{bmatrix} A-sI & B_2 \\ C_1 & D_{12} \end{bmatrix}$ has full column rank for every $s = j\omega$.
5. The pair (A, B_1) has no uncontrollable modes on the imaginary axis.
6. The pair (A, C_1) has no unobservable modes on the imaginary axis.

Theorem 4.6.1 *There exists an admissible controller such that $\|T_{zw}\|_\infty < \gamma$ iff the following conditions hold: [31]*

1. $H_\infty \in \text{dom}(\text{Ric})$ and $X_\infty := \text{Ric}(H_\infty) \geq 0$;
2. $J_\infty \in \text{dom}(\text{Ric})$ and $Y_\infty := \text{Ric}(J_\infty) \geq 0$;
3. $\rho(X_\infty Y_\infty) < \gamma^2$

When the above conditions hold, one such controller is

$$K_{\text{sub}}(s) := \left[\begin{array}{c|c} \hat{A}_\infty & -Z_\infty L_\infty \\ \hline F_\infty & 0 \end{array} \right] \quad (4.43)$$

where

$$\begin{aligned} \hat{A}_\infty &:= A + \gamma^{-2} B_1 B_1^* X_\infty + B_2 F_\infty + Z_\infty L_\infty C_2 \\ F_\infty &= -B_2^* X_\infty, \quad L_\infty = -Y_\infty C_2^*, \quad Z_\infty = (I - \gamma^{-2} Y_\infty X_\infty)^{-1} \end{aligned}$$

4.6.1 Simulation Results

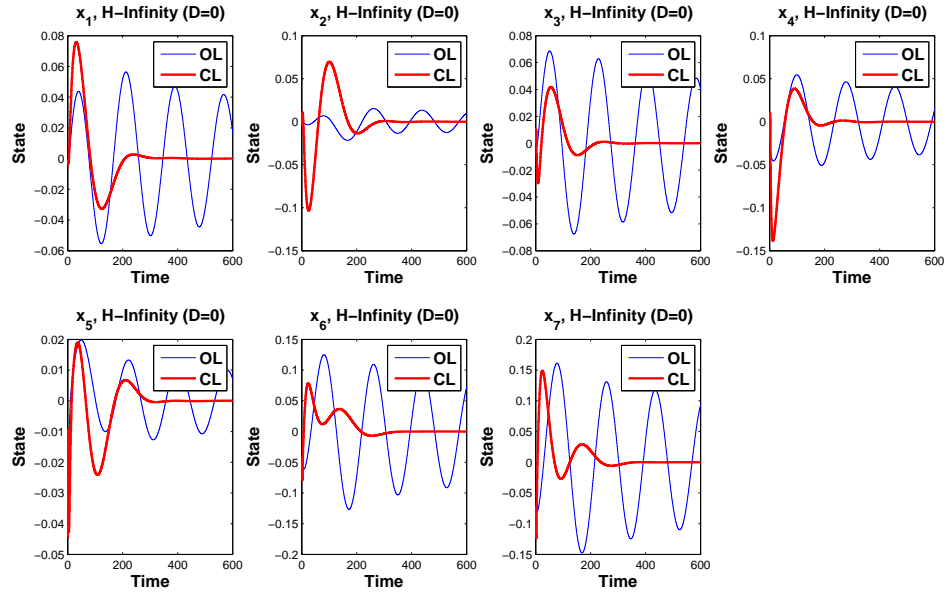
The \mathcal{H}_∞ controller is designed in MATLAB using the function “hinfsyn()”. This function computes a stabilizing output feedback \mathcal{H}_∞ optimal controller and returns it as K . It also computes the closed-loop system T_{zw} , the ∞ -norm or \mathcal{H}_∞ cost of the closed-loop system (i.e., $\gamma = \|T_{zw}\|_\infty$), additional output information and returns these values in CL , Gam , and $Info$ respectively as shown below.

$$[K, CL, Gam, Info] = hinfsyn(G, Ny, Nu)$$

First, through trial and error of the value of D_{12} , stabilizing results were obtained at $D_{12} = 23.6 * I_{6 \times 3}$. Then, further simulations were carried out by fixing the value of D_{12} at $23.6 * I_{6 \times 3}$ and varying the value of D_{21} . The system response has been analyzed for five different values of D_{21} . The \mathcal{H}_∞ norm of the closed-loop system obtained for these five different cases is shown in table 4.4. The state trajectories of the closed-loop system for case 1, 2 and 3 is illustrated in figure 4.11. From the response of the system and the \mathcal{H}_∞ norm of the closed-loop system, it can be concluded that the \mathcal{H}_∞ controller performs best at $D_{12} = 23.6 * I_{6 \times 3}$ and $D_{21} = 10^{-5} * I_{6 \times 6}$. The state trajectories and output trajectories of the open-loop and closed-loop system (with $D_{12} = 23.6 * I_{6 \times 3}$ and $D_{21} = 10^{-5} * I_{6 \times 6}$) are shown in figures 4.11 and 4.12.

Table 4.4: \mathcal{H}_∞ Norm

Case	D_{21}	$\ T_{zw}\ _\infty$
1.	$10^{-5} * I_{6 \times 6}$	0.0096
2.	$10^{-4} * I_{6 \times 6}$	0.0096
3.	$10^{-3} * I_{6 \times 6}$	0.0096
4.	$10^{-2} * I_{6 \times 6}$	0.0191
5.	$10^{-1} * I_{6 \times 6}$	0.1052

Figure 4.11: \mathcal{H}_∞ Control: State Trajectories of OL & CL Systems

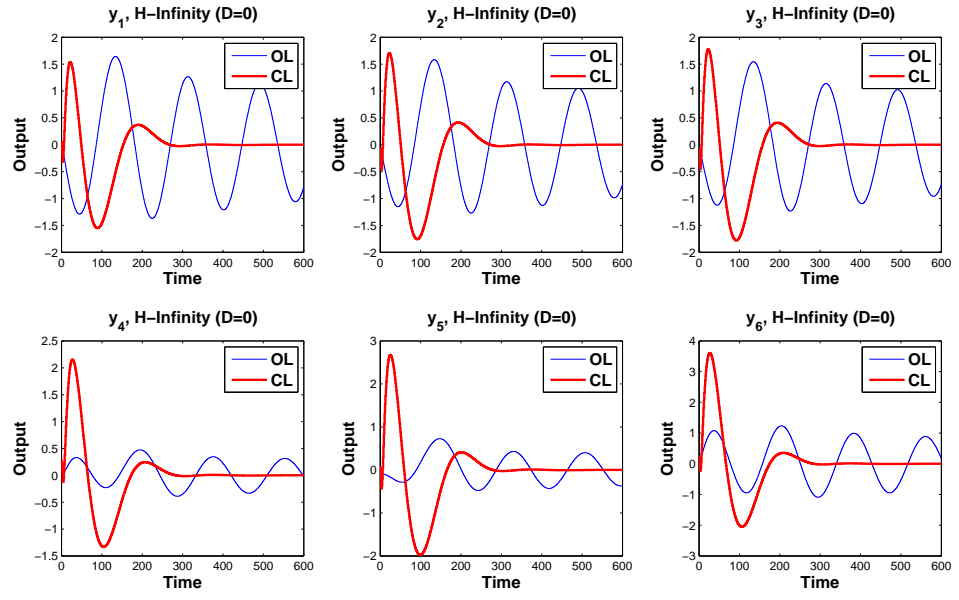


Figure 4.12: \mathcal{H}_∞ Control: Output Trajectories of OL & CL Systems

4.7 Comparison of LQR, LQGR, \mathcal{H}_2 , and \mathcal{H}_∞

Optimal and robust controllers (LQR, LQGR, \mathcal{H}_2 and \mathcal{H}_∞ controllers) are designed for the identified glass furnace model and simulations have been carried using the MATLAB and SIMULINK environment. The closed-loop responses (output trajectories) of the glass furnace system controlled via these techniques are illustrated in figures 4.13 and 4.14.

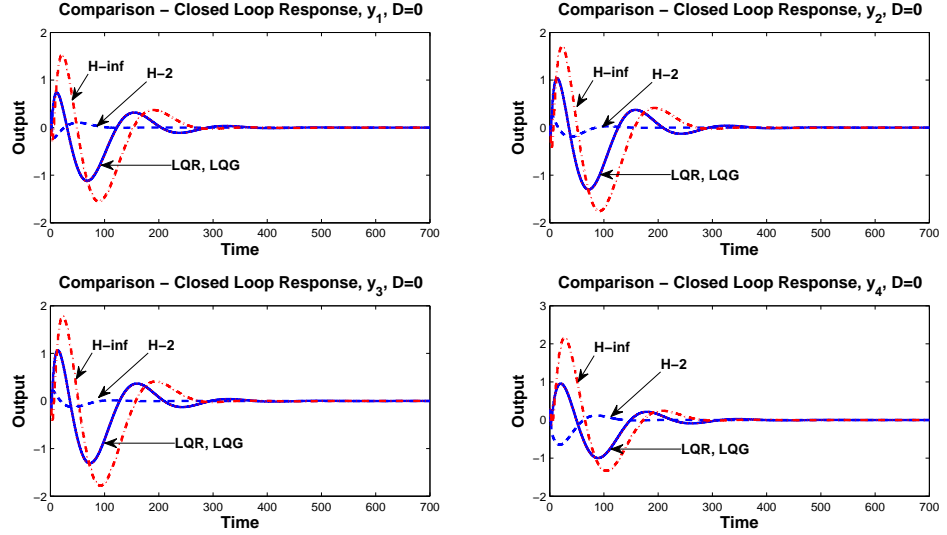


Figure 4.13: Comparison of LQR, LQGR, \mathcal{H}_2 , & \mathcal{H}_∞ : Outputs $y_1 - y_4$

The following observations are deduced from the comparison plots shown in figures 4.13 and 4.14

- With \mathcal{H}_2 controller there is very less amount of overshoot in the output and the settling time is also relatively less.
- The output experiences a large overshoot with \mathcal{H}_∞ controller.

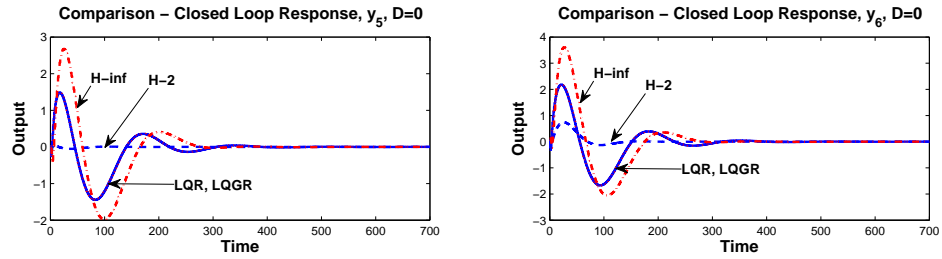


Figure 4.14: Comparison of LQR, LQGR, \mathcal{H}_2 , & \mathcal{H}_∞ : Outputs $y_5 - y_6$

- The response of LQR and LQGR is exactly same and is better than the \mathcal{H}_∞ controller response.

Among the four controllers discussed in this chapter, the \mathcal{H}_2 controller provides best closed-loop performance for the identified glass furnace model.

Chapter 5

MODEL PREDICTIVE CONTROL & ADAPTIVE CONTROL

5.1 Model Predictive Control

5.1.1 Introduction

Model predictive control (MPC) is an advanced control method based on prediction and optimization. This control technique makes use of a model of the process (to be controlled) for computing the future optimal control actions.

MPC systems are used for advanced control of multi-variable processes and for simultaneously maintaining the process variables (controlled variables) and the manipulated variables in certain predefined ranges (i.e., MPC has the ability to handle constraints in a multi-variable control framework). For processes with strong interaction between different signals MPC can offer substantial performance improvement compared with traditional single-input single-output control strategies [34]. Thus, MPC is used widely in many process industry applications.

The following characteristics of MPC make it attractive to both industries and academics [35].

1. MPC uses a completely multi-variable system framework where the performance parameters of the multivariable control system are related to the engineering aspects of the system.
2. It can handle *soft constraints* as well as *hard constraints* in a multivariable control framework. This makes it useful in industries where tight profit margins and limits on the process operation are required.
3. It supports on-line process optimization.
4. It has a simple design framework for handling all these complex issues.
5. It is relatively easy to tune a model predictive controller.
6. It can be used in either supervisory or primary control modes.

Initially, MPC was developed to serve the control needs of power plants and petroleum industry. Due to the aforementioned characteristics of MPC, its use

became widespread over the decades and now it is being used in a wide variety of industries such as food processing, chemical, automotive, aerospace, glass manufacturing industries, etc. After PID control, MPC is the most widely implemented advanced process control methodology in process industries.

In glass manufacturing industry, MPC is used to control glass temperature, crown temperature and bottom temperature in melting furnace, refiner and forehearth. The glass melting process which is carried out in melting furnace exhibits very slow process dynamics; usually it has a response time of several hours. Model predictive control performs well for such processes, because it consistently updates and keeps track of all applied changes in heating/cooling adjustments, and they work out on all individual glass temperatures taking into consideration the full history of process manipulations over several shifts.

The block diagram of model predictive controller is illustrated in figure 5.1.

5.1.2 MPC Algorithm

Model predictive control refers to a class of computer control algorithms that computes sequence of control signals based on the predicted outputs, in order to optimize the response of the plant. The model predictive control algorithm involves a certain number of steps which are as follows:

Initially, a dynamic model of the process is obtained. As the model is used for the prediction of future outputs, it should be noticed that the dynamic model

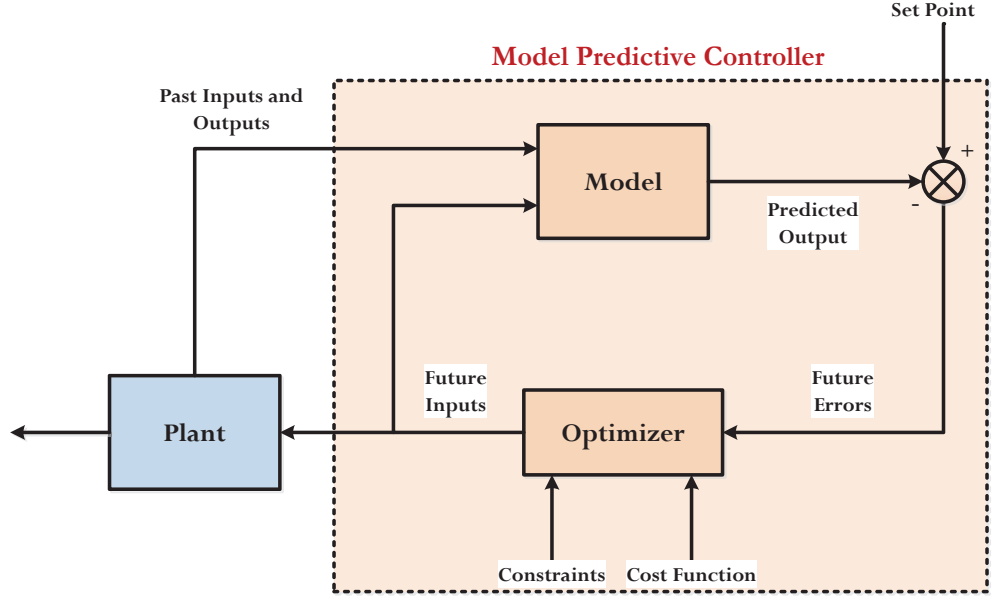


Figure 5.1: Block Diagram of Model Predictive Controller

of the process describes the process well enough so as to obtain consistent and accurate prediction of the future outputs.

1. **Prediction of future outputs:** At time instant n , utilizing the model of the process, and process measurements (past inputs and past outputs), the future behavior of the process outputs (that are to be controlled) is predicted over a certain time horizon known as *prediction horizon* (N_p).

Predicted Output Trajectory

$$= [\hat{y}(n+1), \hat{y}(n+2), \dots, \hat{y}(n+N_p)] \quad (5.1)$$

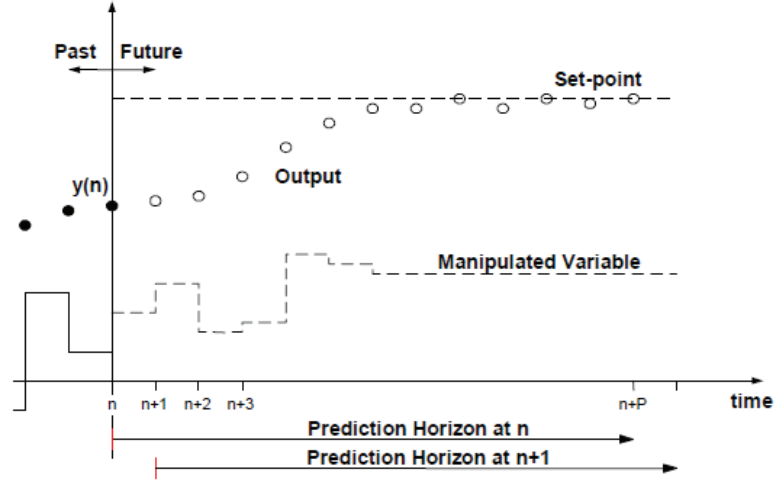


Figure 5.2: Strategy of MPC

2. ***Computing optimum control signals:*** Then based upon these predicted outputs, a sequence of control signals (manipulated variables) that would optimize the future behavior of the process, is generated.

The optimization involves the minimization of the error between the predicted output and the desired output. The constraints on the manipulated variables and the controlled variables are also taken into account in this optimization process. This optimization criteria is expressed as a linear quadratic function of square of the error and square of the control effort required to minimize this error. This function is known as cost function or objective function and it is given by (5.2).

$$J = \sum_{i=1}^{N_p} e(n+i)^T Q e(n+i) + \sum_{i=1}^{N_c} \Delta u(n+i)^T R \Delta u(n+i) \quad (5.2)$$

where $e(n) = (r(n) - \hat{y}(n))$ is the error at time instant n , r is the desired output, \hat{y} is the predicted output, Q and R are the weighting matrices and they are positive definite.

The control signal that minimizes this cost function is determined by carrying out the optimization process within the optimization window N_p .

Optimum Control Trajectory

$$= [u(n), u(n+1), \dots, u(n+(N_c-1))] \quad (5.3)$$

where N_c is known as *control horizon* and it represents the number of parameters used to capture the future control trajectory. The prediction horizon N_p should always be greater than or equal to the control horizon N_c , i.e., $N_c \leq N_p$.

3. ***Applying the control signal:*** From this sequence of optimum control signals (5.3), only first control signal (at current time) i.e., $u(n)$ is given as input to the process. The remaining control signals of the sequence are discarded, because, if the control sequence computed at time instant n is applied over the future horizon N_p , then the possibility of disturbances and modeling errors affecting the process may lead to a decrease in the effectiveness of the computed control signals.

Table 5.1: N_p and N_c

Case	Prediction Horizon N_p	Control Horizon N_c
1.	5	2
2.	10	5
3.	50	5
4.	70	5
5.	100	5
6.	100	10
7.	100	20

4. Next, at time instant $n + 1$, the measurements are taken, the horizon is shifted forward by one step, and the above three steps are repeated. As the computed control signals are implemented in a receding horizon fashion, this control strategy is known as *receding horizon control* or *moving horizon control*.

5.1.3 Simulation Results

Un-constrained MPC

A model predictive controller is designed for the identified glass furnace model, using the MATLAB function “*scmpc*”. The parameters that are used in designing the model predictive controller are N_p , N_c , Q and R . Simulations have been carried out with various combinations of these design parameters as shown in table 5.1.

From these simulations the following observations are deduced. With the

first combination of N_p & N_c , the response is unstable. The response becomes stable with increase in the prediction horizon and the best response is achieved at $N_p = 100$, $N_c = 10$, $Q = [0.25, 0.25, 0.25, 0.25, 0.25, 0.25]$ and $R = [0.1, 0.1, 0.1, 0.1, 0.1, 0.1]$. The output and input trajectories of the closed loop system with these values of controller parameters are presented in figures 5.3 and 5.4.

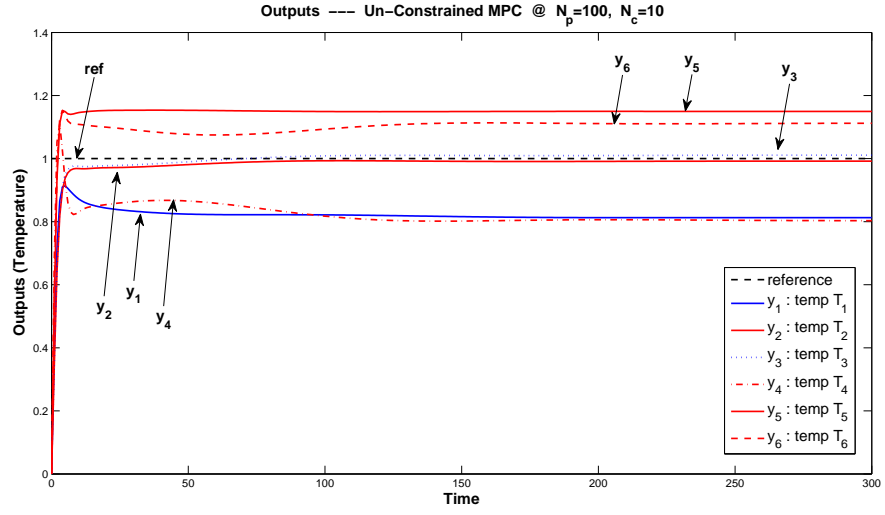


Figure 5.3: Un-constrained MPC: Outputs

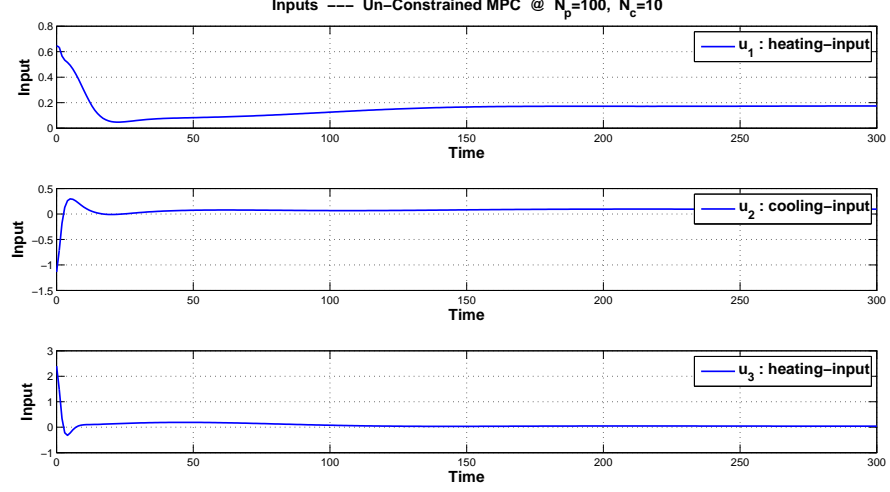


Figure 5.4: Un-constrained MPC: Control Inputs

Constrained MPC

Simulations have been carried out for *constrained* MPC with constraints on inputs and outputs as given by (5.4). The results of constrained MPC are shown in figures 5.5 and 5.6. From the figures, it can be observed that the outputs track the set point while the values of inputs and outputs lie within the constrained limits.

$$\begin{aligned}
 -0.3 \leq u_i \leq 0.3; \quad & i = 1, 2, 3 \\
 0 \leq y_i \leq 1.2; \quad & i = 1, \dots, 6
 \end{aligned} \tag{5.4}$$

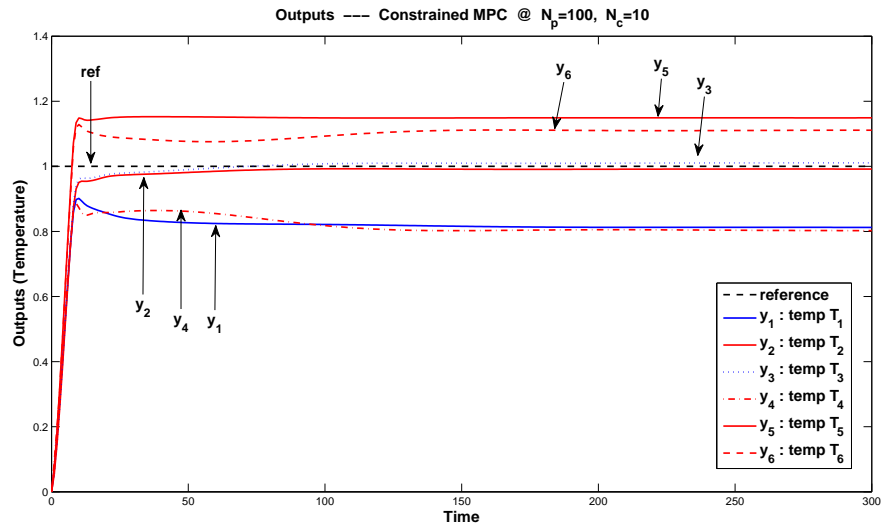


Figure 5.5: Constrained MPC: Outputs

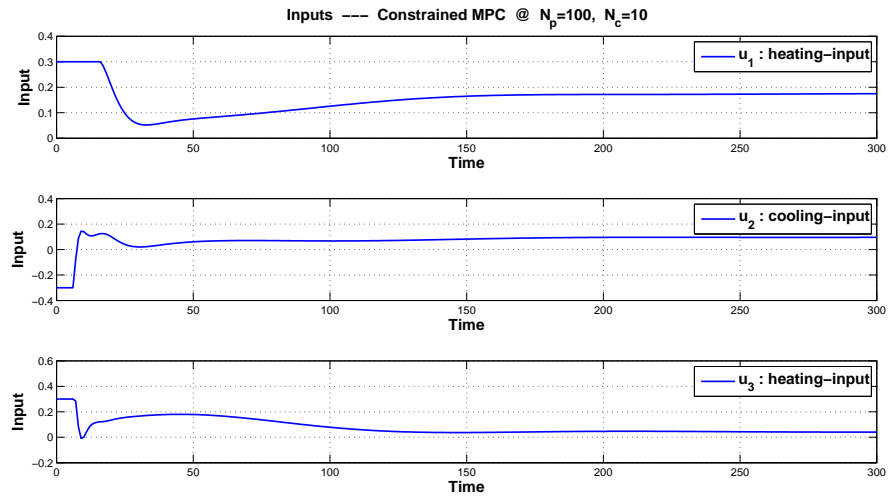


Figure 5.6: Constrained MPC: Control Inputs

5.2 Adaptive Control

5.2.1 Introduction

Adaptive control is a control method in which the controller adapts to the changes in process dynamics (usually the changes that arise due to uncertainty in the process parameters or due to time-varying parameters) and disturbance characteristics. The adjustable parameters and the automatic parameter adjustment mechanism of adaptive controllers help in maintaining a desired level of controller performance in the presence of unknown or time-varying parameters of the dynamic model of the plant. Such controllers are nonlinear in behavior due to the parameter adjustment mechanism. An adaptive control system consists of two loops: an inner loop and an outer loop. The inner loop is a normal feedback loop comprising the plant and the controller. Whereas, the outer loop consists of mechanism for adjusting the parameters of the controller based upon the changes in the process parameters. This loop is known as parameter adjustment loop or the adaptation loop and it is often slower than the normal feedback loop [36].

Adaptive controller is a combination of control law (which is based on the known parameters) and online parameter estimation (through which unknown parameters are estimated at each instant) [37]. This online parameter estimator is known as adaptive law or update law, or adjustment mechanism. Based on the way of combining the control law and the adaptation law, the adaptive con-

trol can be categorized into two types as *direct* adaptive control and *indirect* adaptive control.

In *direct adaptive control*, the plant model is parameterized in terms of the controller parameters that are estimated directly without intermediate calculations involving plant parameter estimates [37] i.e., the controller parameters are changed directly without determining the characteristics of the process and its disturbances.

In *indirect adaptive control*, first the plant parameters are estimated on-line and then these estimates are used to design the controller parameters.

The adaptive law can be designed by using either of the following methods

- Sensitivity methods (MIT-rule)
- Positivity and Lyapunov design
- Gradient method and least-squares methods based on estimation error cost criteria

The following sections present the \mathcal{L}_1 adaptive control theory, its architecture and its implementation on the identified glass furnace model. The “*direct model-reference adaptive control (MRAC) with state predictor*” shown in figure 5.7 is used as a basic architecture for the development of \mathcal{L}_1 adaptive controller. The advantage of using the \mathcal{L}_1 adaptive controller is illustrated by comparing the simulation results of \mathcal{L}_1 adaptive control and MRAC.

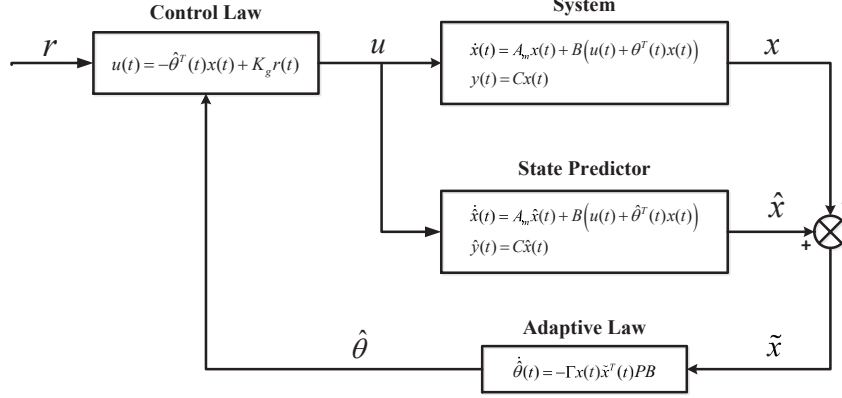


Figure 5.7: Direct MRAC with State Predictor

5.2.2 \mathcal{L}_1 Adaptive Control

A new adaptive control theory that guarantees robustness with fast adaptation was developed by C. Cao and Naira Hovakimyan in 2006 [38]. This type of adaptive control is termed as \mathcal{L}_1 adaptive control and it is basically a modified version of MRAC. In MRAC, the use of high adaptation gain results in high gain feedback control which further results in high-frequency oscillations in the control signal and reduced tolerance to time delays [39]. Also, proper tuning (selection of appropriate adaptive gain) of MRAC is a difficult task. The \mathcal{L}_1 adaptive control method considers uniform performance bounds on the \mathcal{L}_∞ -norms of the errors in model states and control signals. As these error norms are (uniformly) inversely proportional to the square root of the adaptation gain, this method enables the use of high adaptation gains. The \mathcal{L}_1 adaptive control architecture consists of direct MRAC and a bandwidth-limited filter as shown in figure 5.8. The filter is used for the filtering of control signal in order to

avoid high frequencies in the control signal and also for shaping the nominal response. In adaptive control, though the increase in adaptation rate improves the tracking performance, it degrades the robustness of the controller. Hence the adaptation rate is the key to trade-off between performance and robustness. \mathcal{L}_1 adaptive control theory deals with this problem by setting up an architecture that separates the adaptation and robustness and thereby guarantees the transient performance and robustness in the presence of fast adaptation, without introducing or enforcing persistence of excitation, without any gain scheduling in the controller parameters, and without resorting to high-gain feedback [39].

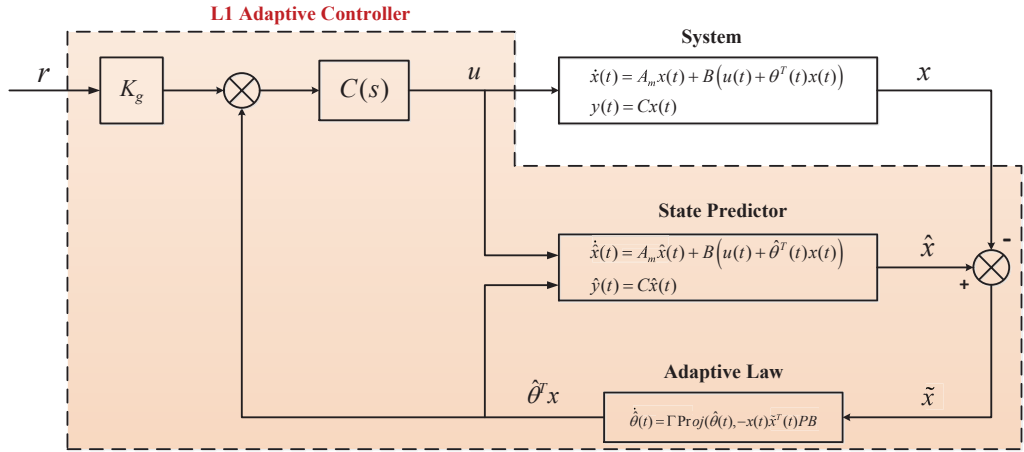


Figure 5.8: Closed Loop \mathcal{L}_1 Adaptive System

The preliminaries of \mathcal{L}_1 adaptive control are given in Appendix.

5.2.3 Problem Formulation

Let the dynamics of a multi-input multi-output (MIMO) system be represented as [39]

$$\begin{aligned} \dot{x}(t) &= Ax(t) + B[u(t) + \theta^T x(t)], & x(0) &= x_0 \\ y(t) &= Cx(t) \end{aligned} \tag{5.5}$$

where $x(t) \in \Re^n$ is the state vector, $u(t) \in \Re$ is the input vector, $y(t) \in \Re$ is the output vector; $A \in \Re^{n \times n}$ is the known state matrix, $B \in \Re^{n \times m}$ is the known input matrix, $C \in \Re^{q \times n}$ is the known output matrix, with (A, B) controllable; θ is the unknown parameter, belonging to a given compact convex set $\theta \in \Theta \subset \Re^{n \times m}$.

\mathcal{L}_1 Adaptive Control Architecture

Let us consider the control architecture (control signal) of the \mathcal{L}_1 adaptive control as a combination of two control signals as shown in (5.6), one control signal u_m to achieve the desired closed loop performance and the other control signal u_{ad} to make the system adaptive to the unknown parameters.

$$u(t) = u_m(t) + u_{ad}(t), \quad u_m(t) = -K_m x(t) \tag{5.6}$$

where $K_m \in \mathbb{R}^{m \times n}$ is the static state feedback gain that leads to a partially closed loop system given by (5.7), with the matrix $A_m = A - BK_m$ being *Hurwitz*; u_{ad} is the adaptive control signal. Substituting the control signal $u(t)$ given by (5.6) in (5.5), we have

$$\begin{aligned} \dot{x}(t) &= A_m x(t) + B[\theta^T x(t) + u_{ad}(t)], & x(0) &= x_0 \\ y(t) &= Cx(t) \end{aligned} \quad (5.7)$$

Let the state predictor for the linearly parameterized system (5.7) be represented as

$$\begin{aligned} \dot{\hat{x}}(t) &= A_m \hat{x}(t) + B[\hat{\theta}^T x(t) + u_{ad}(t)], & \hat{x}(0) &= x_0 \\ \hat{y}(t) &= C\hat{x}(t) \end{aligned} \quad (5.8)$$

where $\hat{x}(t) \in \mathbb{R}^n$ is the state of the predictor and $\hat{\theta}(t) \in \mathbb{R}^{n \times m}$ is the estimate of the parameter θ , governed by the following projection-type adaptive law given by (5.9) [39]

$$\dot{\hat{\theta}}(t) = \Gamma Proj\left(\hat{\theta}(t), -x(t)\tilde{x}^T(t)PB\right), \quad \hat{\theta}(0) = \hat{\theta}_0 \in \Theta \quad (5.9)$$

where $\tilde{x}(t) = \hat{x}(t) - x(t)$ is the prediction error, $\Gamma \in \mathbb{R}^+$ is the adaptation gain, P is the solution of the algebraic Lyapunov equation $A_m^T P + P A_m + Q = 0$ with Q being an arbitrary positive definite symmetric matrix, i.e., $Q = Q^T > 0$. The

projection is confined to the set Θ . The Laplace transform of the adaptive control signal is given as [39]

$$u_{ad}(s) = -C(s) \left[\hat{\eta}(s) - K_g r(s) \right] \quad (5.10)$$

where $r(s)$ is the Laplace transform of the reference signal $r(t)$; $\hat{\eta}(s)$ is the Laplace transform of $\hat{\eta}(t) = \hat{\theta}^T(t)x(t)$; $K_g = -1/(CA_m^{-1}B)$; and $C(s)$ is a BIBO-stable and strictly proper transfer function with DC gain $C(0) = 1$, and its state-space realization assumes zero initialization.

Here, *Lyapunov stability theory* is used to derive these update laws and show convergence criterion (typically persistent excitation), and the *projection* is used to improve the robustness of estimation algorithms. Figure 5.8 illustrates the \mathcal{L}_1 adaptive controller architecture.

The \mathcal{L}_1 adaptive controller is defined by the relationships in (5.6), (5.8), (5.9), and (5.10), with K_m and $C(s)$ verifying the \mathcal{L}_1 norm condition given by the equation (5.11) [39]

$$\lambda = \|G(s)\|_{\mathcal{L}_1} L < 1 \quad (5.11)$$

where

$$G(s) = H(s)(1 - C(s)), \quad H(s) = (sI - A_m)^{-1}B, \quad L = \max_{\theta \in \Theta} \|\theta\|_1 \quad (5.12)$$

5.2.4 Analysis of \mathcal{L}_1 Adaptive Controller

Transient and Steady-State Performance

The prediction error dynamics is obtained from (5.7) and (5.8) as follows [39]

$$\dot{\tilde{x}}(t) = A_m \tilde{x}(t) + B[\tilde{\theta}^T x(t)], \quad \tilde{x}(0) = x_0 \quad (5.13)$$

where $\tilde{x}(t) = \hat{x}(t) - x(t)$ and $\tilde{\theta}(t) = \hat{\theta}(t) - \theta(t)$.

Lemma 5.2.1 *The prediction error represented in (5.13) is uniformly bounded as*

$$\|\tilde{x}\|_{\mathcal{L}_\infty} \leq \sqrt{\frac{\theta_{max}}{\lambda_{min}(P)\Gamma}}, \quad \theta_{max} = 4 \max_{\theta \in \Theta} \|\theta\|^2 \quad (5.14)$$

where $\lambda_{min}(P)$ is the minimum eigen value of P .

Proof: Let us consider the following Lyapunov function candidate

$$V(\tilde{x}(t), \tilde{\theta}(t)) = \tilde{x}^T(t) P \tilde{x}(t) + \frac{1}{\Gamma} \tilde{\theta}^T(t) \tilde{\theta}(t) \quad (5.15)$$

The derivative of this Lyapunov function can be upper bounded along the trajectories of the system, by using the property of the projection operator, as follows [39]

$$\begin{aligned}
\dot{V}(t) &= \dot{\tilde{x}}^T(t)P\tilde{x}(t) + \tilde{x}^T(t)P\dot{\tilde{x}}(t) + \frac{1}{\Gamma} \left(\dot{\tilde{\theta}}^T(t)\tilde{\theta}(t) + \tilde{\theta}^T(t)\dot{\tilde{\theta}}(t) \right) \\
&= \tilde{x}^T(t)(A_m^T P + P A_m)\tilde{x}(t) + 2\tilde{x}^T(t)PB\tilde{\theta}^T(t)x(t) + \frac{2}{\Gamma}\tilde{\theta}^T(t)\dot{\tilde{\theta}}(t) \\
&= -\tilde{x}^T(t)Q\tilde{x}(t) + 2\tilde{x}^T(t)PB\tilde{\theta}^T(t)x(t) + 2\tilde{\theta}^T(t)x(t)Proj\left(\hat{\theta}(t), -x(t)\tilde{x}^T(t)PB\right) \\
&= -\tilde{x}^T(t)Q\tilde{x}(t) + 2\tilde{\theta}^T(t) \left(x(t)\tilde{x}^T(t)PB + Proj\left(\hat{\theta}(t), -x(t)\tilde{x}^T(t)PB\right) \right) \\
&\leq -\tilde{x}^T(t)Q\tilde{x}(t)
\end{aligned}$$

This implies that $\tilde{x}(t)$ and $\tilde{\theta}(t)$ are uniformly bounded. As $\tilde{x}(0) = 0$ we have

$$\lambda_{min}(P)\|\tilde{x}(t)\|^2 \leq V(t) \leq V(0) = \frac{\tilde{\theta}^T(0)\tilde{\theta}(0)}{\Gamma} \quad (5.16)$$

The projection operator ensures that $\hat{\theta}(t) \in \Theta$, and hence

$$\frac{\tilde{\theta}^T(0)\tilde{\theta}(0)}{\Gamma} \leq \frac{4 \max_{\theta \in \Theta} \|\theta\|^2}{\Gamma} \quad (5.17)$$

This leads to the following upper bound

$$\|\tilde{x}(t)\|^2 \leq \frac{\theta_{max}}{\lambda_{min}(P)\Gamma} \quad (5.18)$$

Since $\|\cdot\|_\infty \leq \|\cdot\|$, and as this bound is uniform, the bound given above yields

$$\|\tilde{x}_\tau\|_{\mathcal{L}_\infty} \leq \sqrt{\frac{\theta_{max}}{\lambda_{min}(P)\Gamma}} \quad \forall \tau \geq 0 \quad (5.19)$$

5.2.5 Design of the \mathcal{L}_1 Adaptive Controller: Robustness and Performance

Let us consider the following LTI system with its output free of uncertainties.

Let this system be referred as *design system* [39].

$$x_{des}(s) = C(s)K_g H(s)r(s) + x_{in}(s) \quad (5.20a)$$

$$u_{des}(s) = K_g C(s)r(s) - C(s)\theta^T x_{des}(s) - K_m^T x_{des}(s) \quad (5.20b)$$

$$y_{des}(s) = Cx_{des}(s) \quad (5.20c)$$

where $x_{in}(s) = (sI - A_m)^{-1}x_0$

Lemma 5.2.2 *Subject to (5.11), the following upper bounds hold*

$$\begin{aligned} \|y_{des} - y_{ref}\|_{\mathcal{L}_\infty} &\leq \frac{\lambda}{1-\lambda} \|C\|_1 \left(\|K_g H(s)C(s)\|_{\mathcal{L}_1} \|r\|_{\mathcal{L}_\infty} + \|x_{in}\|_{\mathcal{L}_\infty} \right) \\ \|x_{des} - x_{ref}\|_{\mathcal{L}_\infty} &\leq \frac{\lambda}{1-\lambda} \left(\|K_g H(s)C(s)\|_{\mathcal{L}_1} \|r\|_{\mathcal{L}_\infty} + \|x_{in}\|_{\mathcal{L}_\infty} \right) \\ \|u_{des} - u_{ref}\|_{\mathcal{L}_\infty} &\leq \frac{\lambda}{1-\lambda} \|C(s)\theta^T + K_m^T\|_{\mathcal{L}_1} \left(\|K_g H(s)C(s)\|_{\mathcal{L}_1} \|r\|_{\mathcal{L}_\infty} + \|x_{in}\|_{\mathcal{L}_\infty} \right) \end{aligned}$$

If $x_{in}(t)$ is considered to be decaying exponentially, then the control objective can be achieved through appropriate selection of the static feedback gain K_m and the low-pass filter $C(s)$. The design of K_m and $C(s)$ needs to ensure that $C(s)CH(s)$ has the desired transient and steady state performance characteristics, while simultaneously guaranteeing a small value of \mathcal{L}_1 norm of the closed

loop system $G(s)$ as given by (5.11). Generally, K_m is selected so that the state matrix A_m specifies desired closed loop dynamics, while the bandwidth-limited filter $C(s)$ is designed to track reference signals and compensate for the undesirable effects of the uncertainties within a prespecified range of frequencies.

If $C(s)$ is a low-pass filter, the system $G(s) = H(s)(1 - C(s))$ can be seen as the cascade of a low-pass system $H(s)$ and a high-pass system $(1 - C(s))$. Then, if the bandwidth of $C(s)$, which approximately corresponds to the cut-off frequency of $(1 - C(s))$, is designed to be larger than the bandwidth of $H(s)$, the resulting $G(s)$ is a “no-pass filter” with small \mathcal{L}_1 -norm. Thus, small value of $\|G(s)\|_{\mathcal{L}_1}$ can be obtained by

- increasing the bandwidth of the low-pass filter $C(s)$ for a given set of closed-loop performance specifications, A_m . This solution leads to small design bounds and, therefore, yields a closed-loop adaptive system with desired behavior. However, low-pass filters with high bandwidths may result in high gain feedback and thus lead to closed-loop systems with overly small robustness margins and susceptible to measurement noise.
- reducing the bandwidth of $H(s)$ by slowing down the eigenvalues of the matrix A_m for a given filter design. With this solution, a certain amount of performance is sacrificed to maintain a desired level of robustness.

5.2.6 Simulation Results

The state space model of the identified glass furnace system without disturbances is

$$\begin{aligned}\dot{x}(t) &= Ax(t) + Bu(t) \\ y(t) &= Cx(t)\end{aligned}\tag{5.22}$$

An uncertainty (unknown parameter) $\theta \in \Re^{7 \times 3}$ is introduced in the above system (5.22) as follows

$$\begin{aligned}\dot{x}(t) &= Ax(t) + B[u(t) + \theta^T x(t)] \\ y(t) &= Cx(t)\end{aligned}\tag{5.23}$$

The design parameters for the \mathcal{L}_1 adaptive controller are the feedback gain K_m , filter $C(s)$ and Γ . Of these parameters K_m and $C(s)$ play a key role.

Table 5.2 and figure 5.9 illustrate the poles of the open loop system and the desired closed loop system.

From the pole-zero plot shown in figure 5.9, it can be observed that most of the poles of the open-loop system are very close to the origin and hence the system is marginally stable. In order to make the system more stable the poles of the system should be shifted more towards the left hand side of the plane. Let the desired poles of the system be as shown in table 5.2. The feedback gain matrix

Table 5.2: Desired Poles of Closed-Loop System

Poles of Open-Loop System	Desired Poles of Closed-Loop System
$-0.3312 + 0.0313i$	-0.15
$-0.3312 - 0.0313i$	-0.3
-0.1148	-0.45
$-0.0007 + 0.0354i$	-0.6
$-0.0007 - 0.0354i$	-0.75
$-0.0119 + 0.0145i$	-0.9
$-0.0119 - 0.0145i$	-1.05

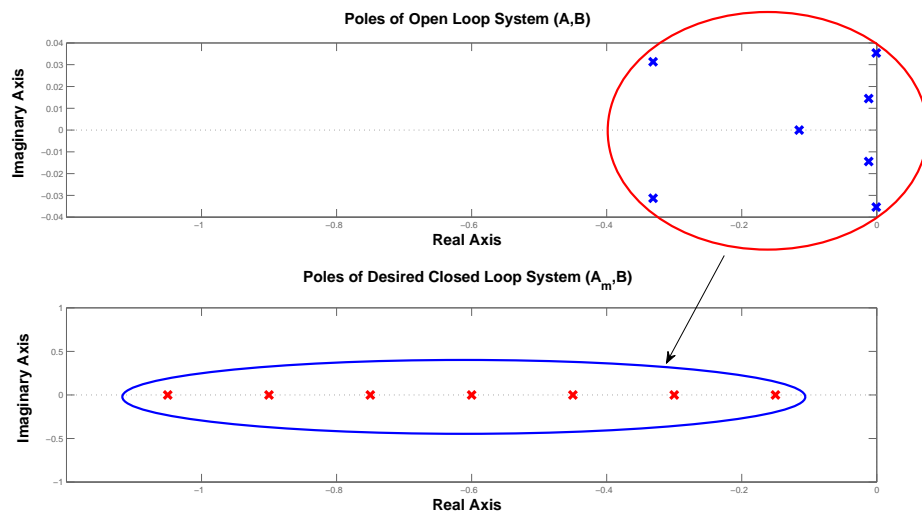


Figure 5.9: Pole-Zero Map of Open-Loop and Desired Closed-Loop System

K_m that leads to a closed-loop system $(A - BK_m)$ with the desired poles shown in table 5.2 is as follows

$$K_m = 10^3 * \begin{bmatrix} 2.6379 & 1.2861 & 5.0086 & -2.4338 & 0.8842 & -2.0053 & 1.1664 \\ 0.5932 & 0.0156 & 6.9388 & -3.8256 & 1.1390 & -0.0230 & -0.7552 \\ -1.7621 & -2.0460 & 3.6611 & -2.5971 & 0.1253 & 1.2761 & -2.0574 \end{bmatrix}$$

The feedforward gain $K_g = -[C(A - BK_m)^{-1}B]^{-1}$ is

$$K_g = \begin{bmatrix} 7.7437 & -44.4479 & -38.3583 & 39.3917 & 4.0909 & 73.8839 \\ 58.1752 & -90.9804 & -73.4638 & 5.2270 & -22.1675 & 130.4167 \\ 71.9771 & -49.2146 & -34.5194 & -33.8663 & -21.0807 & 84.1127 \end{bmatrix}$$

A first order low-pass filter represented by (5.24) is used to filter the control signal $u = K_g r(t) - \hat{\theta}^T(t)x(t)$

$$C(s) = \frac{\omega_c}{s + \omega_c} \quad (5.24)$$

where ω_c is the bandwidth of the filter.

The simulation results of \mathcal{L}_1 adaptive control with the aforementioned design specifications $(K_m, K_g, C(s), \Gamma = 100)$ are as follows:

Figure 5.10 represents the controlled output y_2 for various bandwidths of the low-pass filter $C(s)$ of the \mathcal{L}_1 adaptive controller. The best response is obtained

with a bandwidth $\omega_c = 0.02 \text{ rad/sec}$. From the plots shown in this figure, it is observed that for bandwidths higher than $\omega_c = 0.02 \text{ rad/sec}$, as the bandwidth increases, the overshoot in the response of the system also increases and for bandwidths below this value the response is sluggish.

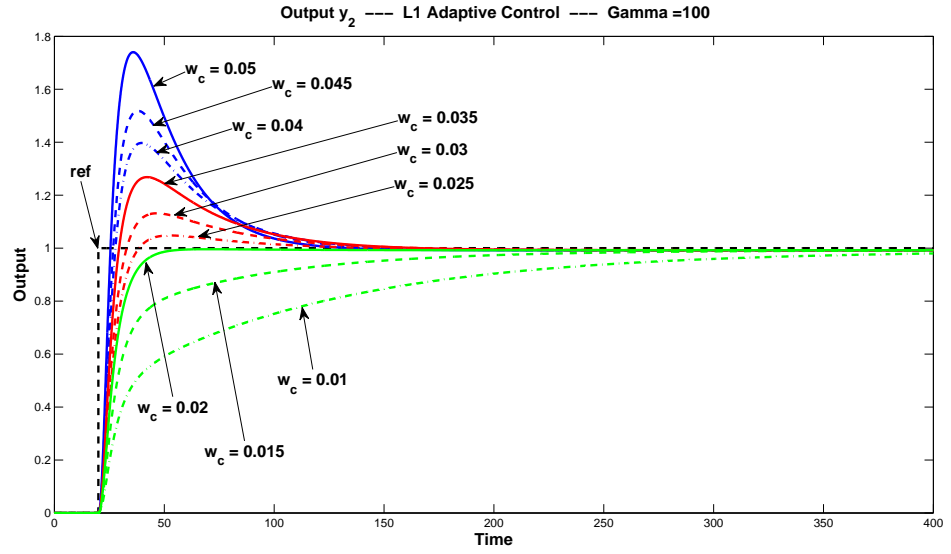
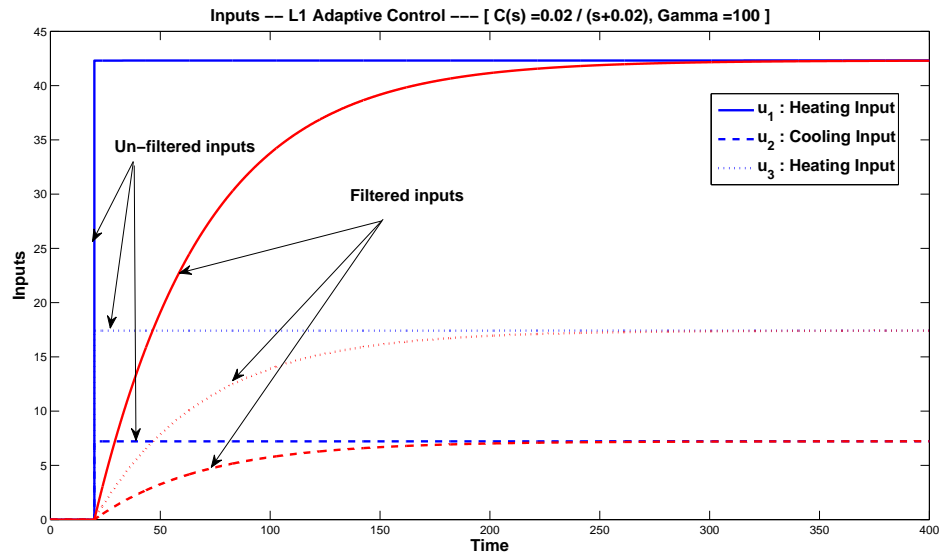
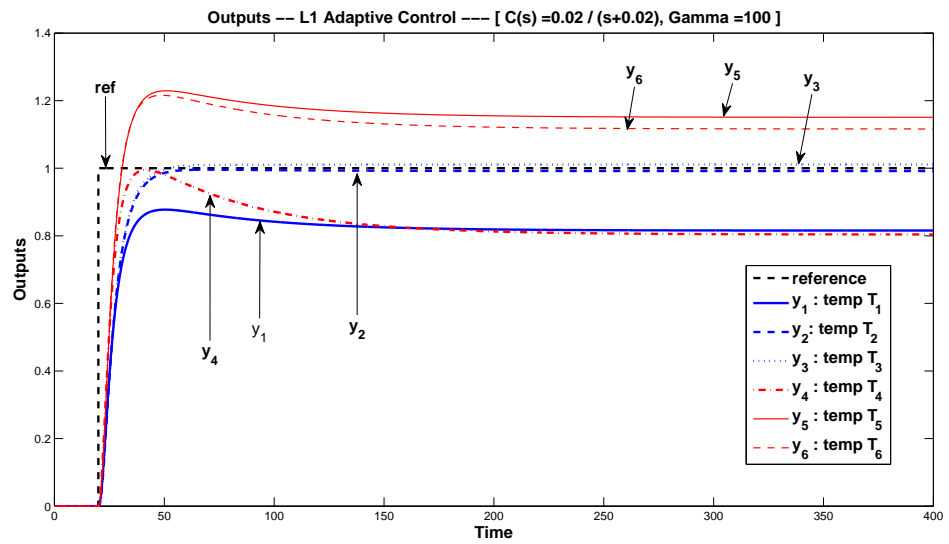


Figure 5.10: Output y_2 with \mathcal{L}_1 Adaptive Control at various filter bandwidths

Figure 5.11 shows the plots of control inputs (unfiltered and filtered) of the \mathcal{L}_1 adaptive controller with the parameters $\omega_c = 0.02 \text{ rad/sec}$, and $\Gamma = 100$. A step input having a magnitude of 1 unit is given as a reference signal. The output trajectories of this closed-loop system are represented in figure 5.12.

Figure 5.11: \mathcal{L}_1 Adaptive System: Control Input TrajectoriesFigure 5.12: \mathcal{L}_1 Adaptive System: Output Trajectories

5.2.7 Comparison of \mathcal{L}_1 Adaptive Control and MRAC

Direct (MRAC) with state predictor has also been applied to this glass furnace model. The closed-loop responses of MRAC system and \mathcal{L}_1 adaptive system are illustrated by control input u_1 and output y_2 in figures 5.13 and 5.14 respectively. It can be seen that the system with \mathcal{L}_1 adaptive controller has a better transient response than the system with MRAC.

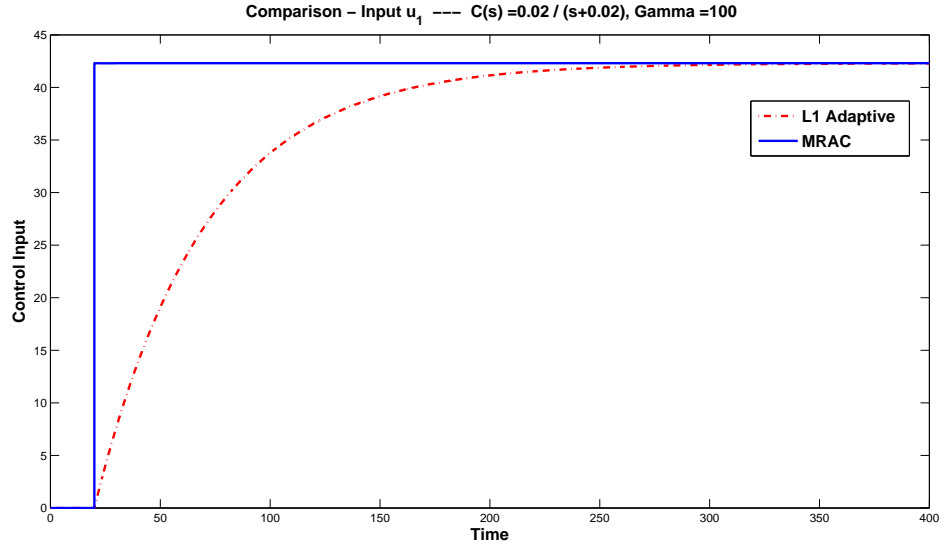


Figure 5.13: \mathcal{L}_1 Adaptive Controller Vs. MRAC: Control Input u_1

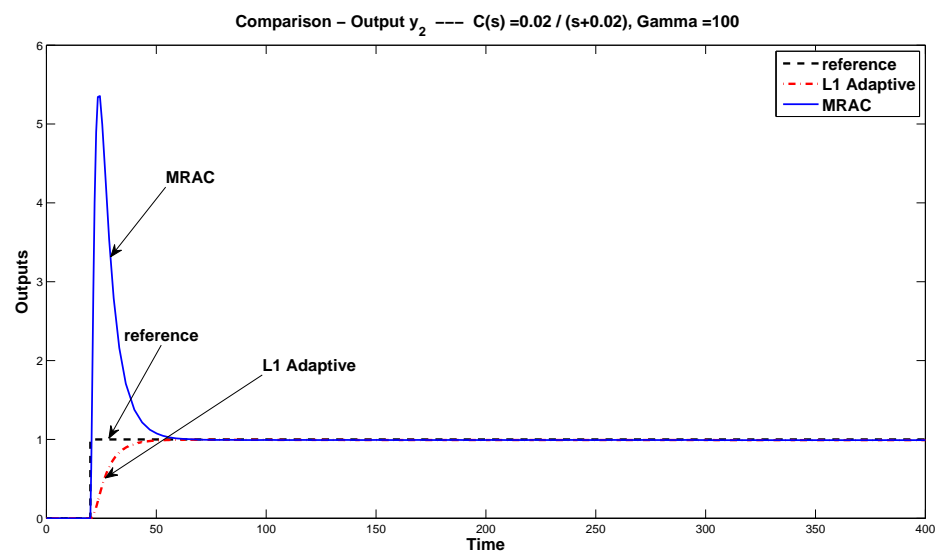


Figure 5.14: \mathcal{L}_1 Adaptive Controller Vs. MRAC: Output y_2

Chapter 6

CONCLUSION AND FUTURE WORK

6.1 Conclusion

Identification of the glass furnace system is performed using the linear identification techniques (prediction error method, N4SID, linear MIMO ARX) and non-linear identification techniques (non-linear MIMO ARX and Hammerstein-Weiner). The models estimated through each of these identification techniques are validated and their model fitness is compared. On comparison, it is found that the models estimated through linear identification techniques have better model fitness, and among the linear models, the PEM model has the best fitness. Initially, the models are estimated assuming that there is no direct feedthrough

from inputs to outputs. Further, from data analysis it is found that there is direct feedthrough from first and third inputs. When the models are estimated again by considering the direct feedthrough from first and third inputs, the fitness of the model improved. Since, the first and third inputs are heating inputs, and the outputs are temperature measures, and as there is an increase in the model fitness when direct feedthrough from these inputs is taken into account, it can be concluded that the real glass furnace system has a direct feedthrough from heating inputs.

The optimal and robust controllers (LQR, LQGR, \mathcal{H}_2 and \mathcal{H}_∞) have been designed and applied to the identified glass furnace model. Implementing these controllers in closed loop with the glass furnace model resulted in satisfying results; \mathcal{H}_2 controller provided the best closed-loop performance.

Model predictive control (MPC), an advanced process control technique, when applied to the glass furnace model produced good results for both the cases: unconstrained case and constrained case (where constraints on input as well as outputs are taken into account).

A new adaptive control technique - \mathcal{L}_1 adaptive control, provided results with good transient response and good robustness characteristics. The results of \mathcal{L}_1 adaptive control are compared with the results of MRAC and it is found that the transient response of \mathcal{L}_1 adaptive system is far better than the transient response of closed loop MRAC system.

6.2 Future Work

The suggestions for possible future work are:

The work in this thesis deals with linear identification and linear control techniques. Since, the glass manufacturing process is a non-linear process, further work can be carried out on non-linear identification and non-linear control techniques (for example, non-linear MPC).

Appendix A

APPENDIX

A.1 PEM model without direct feedthrough

In MATLAB, the “pem()” function computes the prediction error estimate of a general linear model. The following syntax produces a linear state-space model with one delay from the inputs.

$\gg model = pem(data, order) \quad OR$

$\gg model = pem(data, "best");$

The first command line stated above computes a state space model of the order specified by the user. Whereas the second command line with “best” as the

argument computes the state space models for a range of orders 1:10 and then provides a state space model that has best model fitness.

A state space model of the glass furnace without direct feedthrough from input to output (i.e., $D = 0$) is estimated through PEM method using the estimation data set ($zed = 1 - 1200$), through the following MATLAB command line

```
>> pemD=0 = pem(zed, 'best', 'Focus', 'Simulation', 'InitialState', 'Estimate')
```

This produces a 7th order innovation state space model represented as

$$\begin{aligned}x(k+1) &= Ax(k) + Bu(k) + Ke(k) \\ y(k) &= Cx(k) + e(k)\end{aligned}$$

where $A \in \mathbb{R}^{7 \times 7}$, $B \in \mathbb{R}^{7 \times 3}$, $C \in \mathbb{R}^{6 \times 7}$, $K \in \mathbb{R}^{7 \times 6}$, and initial state vector $x(0) \in \mathbb{R}^7$. The numerical values of these parameters are as follows

$$A = \begin{bmatrix} 0.9439 & 0.0237 & 0.0095 & -0.0497 & -0.0077 & -0.0627 & 0.0461 \\ 0.0248 & 0.8714 & 0.0544 & 0.0556 & 0.0661 & 0.2062 & -0.1855 \\ 0.0136 & 0.0178 & 0.9521 & -0.0756 & 0.0746 & 0.0256 & -0.0079 \\ 0.1046 & 0.1248 & -0.1695 & 0.8988 & 0.0162 & -0.1169 & 0.1588 \\ -0.0986 & 0.0648 & 0.0452 & -0.0787 & 0.6713 & -0.3213 & 0.2750 \\ 0.0525 & 0.1193 & -0.0085 & 0.0132 & 0.1297 & 0.9529 & 0.0231 \\ -0.0030 & 0.1103 & 0.0553 & 0.0009 & 0.1209 & -0.0496 & 1.0100 \end{bmatrix}$$

$$B = \begin{bmatrix} -0.0002 & -0.0021 & 0.0041 \\ -0.0003 & 0.0022 & -0.0073 \\ -0.0037 & 0.0058 & 0.0075 \\ -0.0141 & 0.0195 & 0.0082 \\ -0.0115 & 0.0147 & -0.0112 \\ 0.0122 & -0.0188 & 0.0122 \\ 0.0187 & -0.0257 & 0.0133 \end{bmatrix}$$

$$C = \begin{bmatrix} -7.3267 & -24.9670 & -13.4495 & 3.9673 & -1.5981 & 3.1060 & -1.5144 \\ -8.1764 & -25.7989 & -12.2057 & 4.5147 & -0.2547 & -1.7627 & 2.3042 \\ -7.1440 & -25.8632 & -12.3408 & 4.4477 & -0.2661 & -1.8331 & 2.2382 \\ 0.9710 & -21.7385 & 6.1950 & 0.9389 & -4.2347 & -0.1510 & -0.4862 \\ -2.4999 & -29.2818 & -2.3765 & 2.1044 & 0.1200 & -0.6738 & 0.8447 \\ 5.7646 & -26.2680 & 10.8022 & -4.0506 & 2.8262 & 0.2719 & -0.8895 \end{bmatrix}$$

$$K = \begin{bmatrix} 0.0020 & -0.3321 & 0.3209 & -0.0020 & 0.0086 & -0.0016 \\ -0.0035 & 0.1662 & -0.1614 & 0.0058 & -0.0233 & -0.0058 \\ -0.0342 & -0.3801 & 0.3792 & 0.0104 & 0.0087 & -0.0029 \\ -0.0640 & -1.5158 & 1.5410 & 0.0227 & 0.0310 & -0.0748 \\ -0.0267 & 3.4423 & -3.3464 & 0.0038 & -0.0644 & 0.0209 \\ 0.0771 & 6.3629 & -6.4226 & -0.0160 & 0.0161 & 0.0236 \\ 0.0673 & 9.0046 & -9.0331 & -0.0225 & 0.0470 & 0.0277 \end{bmatrix}$$

$$x(0) = \begin{bmatrix} -0.0044 \\ -0.0028 \\ 0.0012 \\ -0.0207 \\ -0.0444 \\ -0.0415 \\ -0.0712 \end{bmatrix}, \quad \text{Eigen Values of } A = \begin{bmatrix} 0.7177 + 0.0225i \\ 0.7177 - 0.0225i \\ 0.8915 \\ 0.9987 + 0.0353i \\ 0.9987 - 0.0353i \\ 0.9880 + 0.0143i \\ 0.9880 - 0.0143i \end{bmatrix}$$

A.2 PEM model with direct feedthrough

A state space model of the glass furnace with direct feedthrough from inputs u_1 and u_3 to outputs (i.e., $D \neq 0$) is estimated through PEM method using the estimation data set ($zed = 1 - 1200$), through the following MATLAB command line

$$\gg pem_{D \neq 0} = pem(zed, 'best', 'Focus', 'Simulation', 'nk', [0 \ 1 \ 0])$$

This produces a 7th order innovation state space model represented as

$$x(k+1) = A_f x(k) + B_f u(k) + K_f e(k)$$

$$y(k) = C_f x(k) + D_f u(k) + e(k)$$

where $A_f \in \mathbb{R}^{7 \times 7}$, $B_f \in \mathbb{R}^{7 \times 3}$, $C_f \in \mathbb{R}^{6 \times 7}$, $D_f \in \mathbb{R}^{6 \times 3}$, $K_f \in \mathbb{R}^{7 \times 6}$, and initial state vector $x_f(0) \in \mathbb{R}^7$. The numerical values of these parameters are as follows

$$A_f = \begin{bmatrix} 1.0057 & 0.0351 & -0.0186 & -0.0184 & -0.0375 & -0.0884 & 0.0685 \\ -0.0105 & 0.9124 & 0.0620 & 0.0668 & 0.0787 & 0.1870 & -0.1739 \\ 0.1001 & 0.0709 & 0.9071 & -0.0410 & 0.0024 & -0.2217 & 0.1902 \\ 0.0951 & 0.0856 & -0.1270 & 0.8747 & -0.0700 & -0.2616 & 0.2705 \\ -0.3436 & -0.1847 & 0.1891 & -0.2424 & 0.7599 & 0.5735 & -0.4200 \\ 0.0276 & 0.1072 & 0.0518 & 0.0311 & 0.0620 & 0.8199 & 0.1150 \\ -0.0993 & 0.0480 & 0.1636 & -0.0021 & 0.0549 & 0.0402 & 0.9268 \end{bmatrix}$$

$$B_f = \begin{bmatrix} -0.0005 & -0.0023 & 0.0024 \\ -0.0002 & 0.0021 & -0.0077 \\ -0.0048 & 0.0056 & 0.0088 \\ -0.0154 & 0.0172 & 0.0092 \\ -0.0100 & 0.0120 & -0.0160 \\ 0.0094 & -0.0162 & 0.0049 \\ 0.0147 & -0.0215 & 0.0006 \end{bmatrix}$$

$$C_f = \begin{bmatrix} -7.2741 & -24.9494 & -13.4544 & 4.0020 & -1.6447 & 3.0439 & -1.4699 \\ -8.0796 & -25.7388 & -12.2649 & 4.5700 & -0.3426 & -1.9007 & 2.4186 \\ -7.2918 & -25.9097 & -12.2602 & 4.4137 & -0.2442 & -1.7143 & 2.1546 \\ 0.9956 & -21.7628 & 6.2225 & 1.0097 & -4.3176 & -0.1908 & -0.4434 \\ -2.5130 & -29.3195 & -2.4093 & 1.9930 & 0.3177 & -0.5358 & 0.7148 \\ 5.7626 & -26.2342 & 10.7996 & -4.0369 & 2.7815 & 0.2230 & -0.8487 \end{bmatrix}$$

$$D_f = \begin{bmatrix} -0.0185 & 0 & 0.2089 \\ 0.0027 & 0 & 0.0952 \\ 0.0029 & 0 & 0.0962 \\ -0.0783 & 0 & 0.6622 \\ -0.0120 & 0 & 0.1236 \\ -0.0097 & 0 & 0.1399 \end{bmatrix}$$

$$K_f = \begin{bmatrix} 0.0142 & -0.4140 & 0.3932 & -0.0061 & -0.0013 & -0.0027 \\ -0.0018 & -0.2131 & 0.2118 & -0.0103 & -0.0138 & -0.0049 \\ -0.0082 & 0.7556 & -0.7555 & 0.0350 & -0.0364 & 0.0174 \\ -0.0082 & 0.4733 & -0.4647 & 0.0098 & -0.0212 & -0.0314 \\ -0.0375 & 1.5266 & -1.4802 & -0.0422 & 0.0223 & 0.0059 \\ 0.0911 & 6.0621 & -6.1311 & -0.0951 & 0.0112 & 0.0167 \\ 0.0906 & 7.8888 & -7.9515 & -0.0977 & 0.0265 & 0.0208 \end{bmatrix}$$

$$x(0)_f = \begin{bmatrix} 0.0010 \\ 0.0017 \\ -0.0086 \\ -0.0014 \\ 0.0081 \\ -0.0358 \\ -0.0386 \end{bmatrix}, \quad \text{Eigen Values of } A_f = \begin{bmatrix} 0.6276 \\ 0.6881 \\ 0.9032 \\ 0.9994 + 0.0354i \\ 0.9994 - 0.0354i \\ 0.9944 + 0.0126i \\ 0.9944 - 0.0126i \end{bmatrix}$$

A.3 Preliminaries of \mathcal{L}_1 Adaptive Control

Definition A.3.1 For a signal $y(t)$, $t > 0$ $y \in \mathbb{R}^n$, its ‘truncated \mathcal{L}_∞ norm’ and ‘ \mathcal{L}_∞ norm’ are given as [38]

$$\|y_t\|_{\mathcal{L}_\infty} = \max_{i=1,\dots,n} \left(\sup_{0 \leq \tau \leq t} |y_i(\tau)| \right) \quad (\text{A.1})$$

$$\|y\|_{\mathcal{L}_\infty} = \max_{i=1,\dots,n} \left(\sup_{\tau \geq 0} |y_i(\tau)| \right) \quad (\text{A.2})$$

Definition A.3.2 The \mathcal{L}_1 gain of an asymptotically stable and proper single-input single-output (SISO) system $H(s)$ is defined as

$$\|H(s)\|_{\mathcal{L}_1} = \int_0^\infty |h(t)| dt \quad (\text{A.3})$$

where $h(t)$ is the impulse response of $H(s)$

Definition A.3.3 The \mathcal{L}_1 gain of an asymptotically stable and proper minput and qoutput system $H(s)$ is defined as

$$\|H(s)\|_{\mathcal{L}_1} = \max_{i=1,\dots,n} \left(\sum_{j=1}^m \|H_{ij}(s)\|_{\mathcal{L}_1} \right) \quad (\text{A.4})$$

Lemma A.3.1 For an asymptotically stable and proper multi-input multi-output (MIMO) system $H(s)$ with input $r(t) \in \mathfrak{R}^m$ and output $x(t) \in \mathfrak{R}^n$, the following holds

$$\|x_t\|_{\mathcal{L}_\infty} \leq \|H(s)\|_{\mathcal{L}_1} \|r_t\|_{\mathcal{L}_\infty} \quad \forall t \geq 0 \quad (\text{A.5})$$

Corollary A.3.1 For an asymptotically stable and proper (MIMO) system $H(s)$, if the input $r(t) \in \mathfrak{R}^m$ is bounded, then the output $x(t) \in \mathfrak{R}^n$ is also bounded, and

$$\|x\|_{\mathcal{L}_\infty} \leq \|H(s)\|_{\mathcal{L}_1} \|r\|_{\mathcal{L}_\infty} \quad (\text{A.6})$$

Lemma A.3.2 For a cascaded system $H(s) = H_2(s)H_1(s)$, where $H_1(s)$ and $H_2(s)$ are asymptotically stable proper systems, the following holds

$$\|H(s)\|_{\mathcal{L}_1} \leq \|H_2(s)\|_{\mathcal{L}_1} \|H_1(s)\|_{\mathcal{L}_1} \quad (\text{A.7})$$

Theorem A.3.1 (\mathcal{L}_1 Small-Gain Theorem) [38]

The interconnected system

$$w_2(s) = \Delta(s) \left(w_1(s) - M(s)w_2(s) \right) \quad (\text{A.8})$$

with input $w_1(t)$ and output $w_2(t)$ is asymptotically stable if

$$\|M(s)\|_{\mathcal{L}_1} \|\Delta(s)\|_{\mathcal{L}_1} < 1 \quad (\text{A.9})$$

Consider a linear time-invariant (LTI) system, $x(s) = (sI - A)^{-1}Bu(s)$ with $A \in \mathbb{R}^{n \times n}$ being a Hurwitz matrix, and let $(sI - A)^{-1}B = n(s)/d(s)$, where $d(s) = \det(sI - A)$ and $n(s)$ is an n -dimensional vector with its i^{th} element being a polynomial function $n_i(s) = \sum_{j=1}^n n_{ij}s^{j-1}$

REFERENCES

- [1] V. Sardeshpande, U. N. Gaitonde, and R. Banerjee, “Model based energy benchmarking for glass furnace,” *Energy Conversion and Management*, vol. 48, issue 10, pp. 2718-2738, 2007.
- [2] M. Un-Chul and K. Y. Lee, “Temperature control of glass melting furnace with fuzzy logic and conventional PI control,” in *American Control Conference, Proceedings of the 2000*, vol.4, pp. 2720-2724, 2000.
- [3] M. CARVALHO, G. and M. NOGUEIRA, “Modelling of glass melting industrial process,” *J. Phys. IV France*, vol. 03, pp. C7-1357-C7-1366, 1993.
- [4] P. Sung Joo and Y. Jin Seol, “Intelligent process control: application of neural network to glass melting furnace control,” in *Expert Systems for Development, Proceedings of International Conference on*, pp. 255-260, 1994.
- [5] B. Gough, P. Eng, and D. Matovich, “Predictive-adaptive temperature control of molten glass,” in *Dynamic Modeling Control Applications for Industry Workshop, IEEE Industry Applications Society*, pp. 51-55, 1997.

- [6] S. R. Venkateswaran, J. L. Conrad, and G. A. Walzer, "Modeling of the glass melting process," in *Industry Applications Society Annual Meeting, Conference Record of the 1990 IEEE*, vol.2, pp. 1343-1348, 1990.
- [7] L. Huisman, "Control of glass melting processes based on reduced CFD models," *PhD Thesis*, Eindhoven University of Technology, Eindhoven, 2005.
- [8] P. Havel, "Overview of automatic control of glass furnaces," *Ceramics - Silikaty*, vol. 50, pp. 51-55, 2006.
- [9] S. P. DABLEMONT and M. R. GEVERS, "Identification and control of a glass-furnace," *Preprints 4th IFAC Symposium on Identification and System Parameter Estimation*, Tbilisi, 1976.
- [10] R. Haber, J. Hetthessy, L. Keviczky, I. Vajk, A. Feher, N. Czeiner, Z. Csaszar, and A. Turi, "Identification and adaptive control of a glass furnace," *Automatica*, vol. 17, pp. 175-185, 1981.
- [11] V. Wertz and P. Demeuse, "Application of Clarke-Gawthrop type controllers for the bottom temperature of a glass furnace," *Automatica*, vol. 23, pp. 215-220, 1987.
- [12] J. Kang-Mo and L. Kang-Suk, "A decision support system using neural networks in a glass furnace process," in *Neural Networks, IJCNN '93-Nagoya. Proceedings of 1993 International Joint Conference on*, vol.3, pp. 2795-2798, 1993.

- [13] M. Un-Chul and K. Y. Lee, "Multi-loop control of temperature for TV glass furnace," in *Decision and Control, 2000. Proceedings of the 39th IEEE Conference on*, vol.5, pp. 4550-4555, 2000.
- [14] H. Zhang, C. Z. Han, B. W. Wan, and R. Shi, "Identification and control of a large kinescope glass furnace," *Automatica*, vol. 30, pp. 887-892, 1994.
- [15] A. R. Holladay, "Modeling and Control of a Small Glass Furnace," *Master's Thesis*, Department of Mechanical Engineering, West Virginia University, 2005.
- [16] H. A. Morris, "Advanced Modeling For Small Glass Furnaces," *Masters's Thesis*, Department of Mechanical Engineering, West Virginia University, 2007.
- [17] S. Liu and L. E. Banta, "Estimator-Based LQR Control Model for Glass Fiber Furnace," *International Journal of Applied Glass Science*, vol. 3, pp. 275-286, 2012.
- [18] O. Auchet, C. Iung, O. Mallasse, and P. Riedinger, "Glass furnace, simplified modelling for control and real time simulation," in *Industrial Electronics, IEEE International Symposium on*, vol. 1, pp. 657-661, 2004.
- [19] T. C. Backx, L. Huisman, P. Astrid, and R. Beerkens, "Model-Based Control of Glass Melting Furnaces and Forehearth: First Principles-Based Model of Predictive Control System Design," in *63rd Conference on Glass Problems: Ceramic Engineering and Science Proceedings*, ed: John Wiley & Sons, Inc., pp. 21-47, 2008.

- [20] R. R. J. J. Schobben, "Identification & CFD Model Based Control of a Glass Furnace," *Master's Thesis*, Department of Electrical Engineering, Eindhoven University of Technology, 2009.
- [21] S. Wattamwar, S. Weiland, and T. Backx, "Identification of low dimensional models for slow geometric parameter variation in an Industrial Glass Manufacturing Process," in *Control Applications, CCA 2008. IEEE International Conference on*, pp. 989-994, 2008.
- [22] O. Auchet, P. Riedinger, O. Malasse, and C. Iung, "First-principles simplified modelling of glass furnaces combustion chambers," *Control Engineering Practice*, vol. 16, pp. 1443-1456, 2008.
- [23] M. Hadjili, A. Lendasse, V. Wertz, and S. Yurkovich, "Identification of fuzzy models for a glass furnace process," in *Control Applications, Proceedings of the 1998 IEEE International Conference on*, vol.2, pp. 963-968, 1998.
- [24] J. M. Pina and P. U. Lima, "A glass furnace operation system using fuzzy modelling and genetic algorithms for performance optimisation," *Engineering Applications of Artificial Intelligence*, vol. 16, issue 10, pp. 681-690, 2003.
- [25] J. H. Hill, B. E. Ydstie, and Y. Jiao, "Adaptive Control of an Industrial Float Glass Process," *IFAC*, 2002.
- [26] J. Qi and G. Ma, "Design of Glass Furnace Control System Based on Model-Free Adaptive Controller," in *Computer Modeling and Simulation, ICCMS '10. Second International Conference on*, pp. 130-133, 2010.

- [27] L. Ljung, *System Identification - Theory for the User, 2nd ed.*: Prentice Hall.
- [28] De Moor B.L.R. (ed.), DaISy: Database for the Identification of Systems, Department of Electrical Engineering, ESAT/SISTA, K.U.Leuven, Belgium, URL: <http://www.esat.kuleuven.ac.be/sista/daisy/>. [Used dataset: *Data of a glass furnace (Philips)*, section: *Process Industry Systems*, code: *96-002*]
- [29] M. S. Mahmoud and Y. Xia, *Applied Control Systems Design*: Springer, 2012.
- [30] W. S. Levine, *The Control Handbook (Second Edition): Control System Advanced Methods*: CRC Press (Taylor and Francis Group, LLC), 2011.
- [31] K. Zhou, J. C. Doyle, and K. Glover, *Robust and Optimal Control*: Prentice Hall, 1996.
- [32] O. H. Bosgra, H. Kwakernaak, and G. Meinsma, *Design Methods for Control Systems*: Notes for a course of the Dutch Institute of Systems and Control (DISC), Winter term 2001/2002.
- [33] J. B. Burl, *Linear Optimal Control - \mathcal{H}_2 and \mathcal{H}_∞ Methods*: Addison Wesley Longman, 1999.
- [34] M. Lundh and M. Molander, “State-Space Models in Model Predictive Control,” *ABB Automation Products AB*.

- [35] L. Wang, *Model Predictive Control System Design and Implementation using MATLAB*: Springer, 2009.
- [36] K. J. Astrom and B. Wittenmark, *Adaptive Control*: Addison-Wesley Publishing Company, 1995.
- [37] P. A. Ioannou and J. Sun, *Robust adaptive control*: PTR Prentice-Hall, 1996.
- [38] C. Chengyu and N. Hovakimyan, “Design and Analysis of a Novel L1 Adaptive Controller, Part I: Control Signal and Asymptotic Stability,” in *American Control Conference*, pp. 3397-3402, 2006.
- [39] N. Hovakimyan and C. Cao, *L1 Adaptive Control Theory: Guaranteed Robustness with Fast Adaptation*: Society for Industrial and Applied Mathematics, 2010.
- [40] T. Backx, J. Ludlage, and A. Koenraads, “Application Of Model Predictive Control For Quality Control Of Glass Melting Processes,” *IPCOS Technology*.
- [41] I. Harmati and B. Lantos, “Adaptive Control and On-line Controller Design for Multivariable Systems in State Space.”
- [42] I. Gustavsson, “Survey of applications of identification in chemical and physical processes,” *Automatica*, vol. 11, pp. 3-24, 1975.
- [43] R. Rouhani and R. K. Mehra, “Model algorithmic control (MAC); basic theoretical properties,” *Automatica*, vol. 18, pp. 401-414, 1982.

- [44] K. J. Astrom, "Theory and applications of adaptive control - A survey," *Automatica*, vol. 19, pp. 471-486, 1983.
- [45] W. Trier, K. L. Loewenstein, and S. o. G. Technology, Glass Furnaces: Design, Construction and Operation: *Society of Glass Technology*, 1987.
- [46] G. S. Black, Jr., "Control technology applied to glass level regulation," in *Industry Applications Society Annual Meeting, Conference Record of the 1988 IEEE*, vol.2, pp. 1111-1117, 1988.
- [47] B. E. Ydstie, A. H. Kemna, and L. K. Liu, "Multivariable extended-horizon adaptive control," *Computers & Chemical Engineering*, vol. 12, pp. 733-743, 1988.
- [48] T. Soderstrom and P. Stocia, *System Identification*: Prentice Hall International, 1989.
- [49] K. Najim and M. M. Saad, "Adaptive control: theory and practical aspects," *Journal of Process Control*, vol. 1, pp. 84-95, 1991.
- [50] T. C. Backx and A. A. H. Damen, "Identification for the control of MIMO industrial processes," *Automatic Control, IEEE Transactions on*, vol. 37, pp. 980-986, 1992.
- [51] V. Wertz, J. F. Simon, and M. Gevers, "Adaptive control of the temperature of a glass furnace," in *Proc. IFAC Symp. on Adaptive Control and Signal Processing*, pp. 555-560, 1992.

- [52] A. J. Thornton and P. F. Ebzery, "Application of adaptive extended horizon control to a pyrometallurgical reactor," *Journal of Process Control*, vol. 4, pp. 91-97, 1994.
- [53] P. Van Overschee and B. De Moor, "N4SID: Subspace algorithms for the identification of combined deterministic-stochastic systems," *Automatica*, vol. 30, pp. 75-93, 1994.
- [54] L. Ljung, *System Identification Toolbox - User's Guide (for use with MATLAB)*: The MathWorks, Inc, 1995.
- [55] R. Babuska and H. B. Verbruggen, "An overview of fuzzy modeling for control," *Control Engineering Practice*, vol. 4, pp. 1593-1606, 1996.
- [56] Q. Wang, G. Chalaye, G. Thomas, and G. Gilles, "Predictive control of a glass process," *Control Engineering Practice*, vol. 5, issue 2, pp. 167-173, 1997.
- [57] W. Favoreel, "Benchmark for subspace system identification algorithms," *Katholieke Universiteit Leuven, Department of Electrical Engineering - ESAT / SISTA*, 1998.
- [58] L. Ljung, "Estimation focus in system identification: prefiltering, noise models, and prediction," in *Decision and Control, Proceedings of the 38th IEEE Conference on*, vol.3, pp. 2810-2815, 1999.
- [59] T. Backx, J. Ludlage, and A. Koenraads, "Model-based process control ensures predictable process operation," *Glass*, vol. 77, pp. 180-182, 2000.

- [60] M. Nikolaou, “Model predictive controllers: A critical synthesis of theory and industrial needs,” in *Advances in Chemical Engineering. vol. Volume 26, ed: Academic Press*, pp. 131-204, 2001.
- [61] L. Huisman, “Estimation of process variables in a glass melting furnace,” *IFAC*, vol. 15th Terminal World Congress, Barcelona, Spain, 2002.
- [62] J. M. Maciejowski, *Predictive Control: With Constraints*: Prentice Hall PTR, 2002.
- [63] S. J. Qin and T. A. Badgwell, “A survey of industrial model predictive control technology,” *Control Engineering Practice*, vol. 11, pp. 733-764, 2003.
- [64] M. Un-Chul and K. Y. Lee, “Hybrid algorithm with fuzzy system and conventional PI control for the temperature control of TV glass furnace,” *Control Systems Technology, IEEE Transactions on*, vol. 11, pp. 548-554, 2003.
- [65] J. Qi, Z. Deng, and Y. Li, “Design of Fuzzy PID Controller and Application in Glass Furnace,” in *Electronic Measurement and Instruments, ICEMI '07. 8th International Conference on*, pp. 4-224-4-227, 2007.
- [66] M. Un-Chul, “A Practical Multiloop Controller Design for Temperature Control of a TV Glass Furnace,” *Control Systems Technology, IEEE Transactions on*, vol. 15, pp. 1137-1142, 2007.
- [67] E. Muysenberg and J. Chmelar, “Validation of Glass Furnace Models: Believe it or Not,” in *A Collection of Papers Presented at the 61st Confer-*

- ence on Glass Problems: Ceramic Engineering and Science Proceedings*, ed: John Wiley & Sons, Inc., pp. 1-19, 2008.
- [68] A. Ponsich, C. Azzaro-Pantel, S. Domenech, L. Pibouleau, and F. Pigeonneau, "A systemic approach for glass manufacturing process modeling," *Chemical Engineering and Processing: Process Intensification*, vol. 48, pp. 1310-1320, 2009.
- [69] P. van Santen, L. Huisman, and S. van Deelen, "Model Based Process Control for Glass Furnace Operation," in *71st Conference on Glass Problems*, ed: John Wiley & Sons, Inc., pp. 203-213, 2011.
- [70] S. Dequan, G. Guili, G. Zhiwei, and X. Peng, "Application of Expert Fuzzy PID Method for Temperature Control of Heating Furnace" *Procedia Engineering*, vol. 29, pp. 257-261, 2012.

VITAE

- Name*** : Mohammed Abdul Hai
- Nationality*** : Indian
- Education*** : Bachelor of Engineering (BE) in *Instrumentation Engineering*, Muffakham Jah College of Engineering and Technology, Osmania University, Hyderabad, India.
- : Master of Science (MS) in *Systems Engineering (with specialization in Automation and Control)*, King Fahd University of Petroleum and Minerals, Dhahran, Saudi Arabia.
- Experience*** : *Research Assistant*, Systems Engineering Department, King Fahd University of Petroleum and Minerals, February 2010 to May 2013.
- Email*** : abdulhai4@gmail.com
- Permanent Address*** : Hyderabad, India.